RÉPUBLIQUE ALGÉRIENNE DÉMOCRATIQUE ET POPULAIRE
MINISTÈRE DE L'ENSEIGNEMENT SUPÉRIEUR ET DE LA RECHERCHE SCIENTIFIQUE
ÉCOLE NATIONALE POLYTECHNIQUE



DÉPARTEMENT DE GÉNIE CIVIL
LABORATOIRE DE GÉNIE PARASISMIQUE ET DE DYNAMIQUE DES STRUCTURES

# Final Year Project Thesis

For the Degree of State Engineer in Civil Engineering

## Hybrid AI-Based Sensor Optimization for Structural Health Monitoring of Multi-story Buildings — Case Study: HQ Tower R+12

**by Mohamed Boukharouba**

**Defended on:** July 01, 2025

**Examination Committee**

| | |
|---|---|
| **President** | Mr. Abdelmadjid Tadjadit Assist. Professor, ENP |
| **Advisors** | Mr. Nouredine Bourahla Professor, ENP |
| | Mr. Abdellatif Hannachi PhD Student, ENP |
| **Examiner** | Mr. Abdelkrim Bourzam Professor, ENP |
| **Guests** | Mrs. Selma Larbi Assist. Professor , ENSTP |
| | Miss Zeghmar Racha Lecturer, ENP |

ENP 2025

RÉPUBLIQUE ALGÉRIENNE DÉMOCRATIQUE ET POPULAIRE
MINISTÈRE DE L'ENSEIGNEMENT SUPÉRIEUR ET DE LA RECHERCHE SCIENTIFIQUE
ÉCOLE NATIONALE POLYTECHNIQUE



DÉPARTEMENT DE GÉNIE CIVIL
LABORATOIRE DE GÉNIE PARASISMIQUE ET DE DYNAMIQUE DES STRUCTURES

# Final Year Project Thesis

For the Degree of State Engineer in Civil Engineering

## Hybrid AI-Based Sensor Optimization for Structural Health Monitoring of Multi-story Buildings — Case Study: HQ Tower R+12

**by Mohamed Boukharouba**

**Defended on:** July 01, 2025

**Examination Committee**

| | |
|---|---|
| **President** | Mr. Abdelmadjid Tadjadit Assist. Professor, ENP |
| **Advisors** | Mr. Nouredine Bourahla Professor, ENP |
| | Mr. Abdellatif Hannachi PhD Student, ENP |
| **Examiner** | Mr. Abdelkrim Bourzam Professor, ENP |
| **Guests** | Mrs. Selma Larbi Assist. Professor , ENSTP |
| | Miss Zeghmar Racha Lecturer, ENP |

ENP 2025

RÉPUBLIQUE ALGÉRIENNE DÉMOCRATIQUE ET POPULAIRE
MINISTÈRE DE L'ENSEIGNEMENT SUPÉRIEUR ET DE LA RECHERCHE SCIENTIFIQUE
ÉCOLE NATIONALE POLYTECHNIQUE



DÉPARTEMENT DE GÉNIE CIVIL
LABORATOIRE DE GÉNIE PARASISMIQUE ET DE DYNAMIQUE DES STRUCTURES

# Mémoire de Projet de Fin d'Études

En vue de l'obtention du diplôme d'Ingénieur d'État en Génie Civil

## Optimisation Hybride de Capteurs basée sur l'IA pour la Surveillance de la Santé des Structures des Bâtiments Multi-étages — Étude de Cas : Tour HQ R+12

**par Mohamed Boukharouba**

**Soutenu le :** 01 Juillet 2025

**Jury d'Examen**

| | |
|---|---|
| **Président** | M. Abdelmadjid Tadjadit Maître de Conférences, ENP |
| **Encadreurs** | M. Nouredine Bourahla Professeur, ENP |
| | M. Abdellatif Hannachi Doctorant, ENP |
| **Examinateur** | M. Abdelkrim Bourzam Professeur, ENP |
| **Invités** | Mme Selma Larbi Maître de Conférences, ENSTP |
| | Mlle Zeghmar Racha Chargée de Cours, ENP |

ENP 2025

# ملخص

تلعب مراقبة صحة المنشآت دورا حاسما في ضمان السلامة ووظائف المنشآت الحيوية مثل الجسور والسدود والمباني العامة. لجعل أنظمة أكثر فعالية من حيث التكلفة، من الضروري تحديد افضل عدد للمستشعرات ومواقعها، مما يقلل تكاليف التنفيذ مع الحفاظ على موثوقية الكشف عن الأضرار وتقييم حالة المنشأة.

تعالج هذه الدراسة مسألة تحسين توزيع المستشعرات المتكفية تجاه الضرر في مراقبة صحة المنشآت للمباني متعددة الطوابق. تم تطوير نموذج عناصر محدودة ثلاثي الأبعاد لبرج خرسانة مسلحة مكون من 12 طابقا (R+12) باستخدام SAP2000، مما أتاح تحديد مناطق الخطر العالية استناداً إلى توزيع القوى الداخلية. تم توليد استجابات اهتزازية في الحالة المستقرة، واستخدمنا خوارزمية وراثية لتحديد التموقع الأمثل للمستشعرات في كل سيناريو من سيناريوهات الضرر باستخدام مصفوفات المسافة كميزات حساسة للضرر. ثم تم دمج هذه التصاميم القائمة على السيناريوهات في تكوين موحد من خلال تحليل تكرار ظهور المستشعرات وقيم أهميتها. يضمن مجموعة المستشعرات النهائية تغطية وحساسية كافيتين لتدهور المنشأة مع الحفاظ على عدد منخفض من المستشعرات.

يوفر النهج المقترح حلا عمليا وقابلاً للتطوير لتصميم أنظمة (SHM) في الهياكل المعقدة ذات مناطق الضرر المتوقعة.



الكلمات المفتاحية: مراقبة صحة المنشآت ، تحسين توزيع المستشعرات، الخوارزمية الوراثية، مصفوفة المسافة، الاستشعار التكيفي للضرر.



# Résumé

La surveillance de la santé des structures (SHM) joue un rôle crucial pour assurer la sécurité et le bon fonctionnement d'infrastructures vitales telles que les ponts, les barrages et les bâtiments publics. Afin de rendre les systèmes SHM plus économiques, il est essentiel d'optimiser le nombre et l'emplacement des capteurs, réduisant ainsi les coûts de mise en œuvre tout en garantissant une détection fiable des dommages et une évaluation structurelle efficace.

Cette étude aborde le problème de l'optimisation d'un agencement de capteurs adaptatif aux dommages pour la surveillance de la santé structurelle des bâtiments à plusieurs étages. Un modèle éléments finis tridimensionnel d'une tour en béton armé de 12 étages (R+12) a été développé à l'aide de SAP2000, permettant d'identifier les zones à haut risque de dommages selon la distribution des efforts internes. Des réponses vibratoires en régime permanent ont été simulées, et un algorithme génétique a été utilisé pour déterminer la configuration optimale de capteurs pour chaque scénario de dommage, en s'appuyant sur des matrices de distances comme caractéristiques sensibles aux altérations. Ces configurations liées à chaque scénario ont ensuite été fusionnées en une configuration unifiée par l'analyse de la fréquence d'apparition et de l'importance des capteurs. L'ensemble final de capteurs assure une couverture et une sensibilité suffisantes à la dégradation structurelle tout en maintenant un nombre réduit de capteurs. L'approche proposée offre une solution pratique et évolutive pour la conception de systèmes SHM dans des structures complexes avec des zones de dommage anticipées.



**Mots-clés :** Surveillance de la santé structurelle, Optimisation des capteurs, Algorithme génétique, Matrice de distances, Détection adaptative des dommages.

# Abstract

Structural Health Monitoring (SHM) plays a critical role in ensuring the safety and functionality of vital structures such as bridges, dams, and public buildings. To make SHM systems more cost-effective, it is essential to optimize the number and placement of sensors, reducing implementation costs while maintaining reliable damage detection and structural assessment.

This study addresses the problem of optimizing damage-adaptive sensor layout in structural health monitoring (SHM) for multi-story buildings. A three-dimensional finite element model of a 12-story reinforced concrete tower (R+12) was developed using SAP2000, enabling the identification of high-risk damage zones based on internal force distributions. Steady-state vibration responses were generated, and a genetic algorithm was used to identify the optimal sensor configuration for each damage scenario using distance matrices as damage-sensitive features. These scenario-based layouts were then merged into a unified configuration by analyzing sensor occurrence and importance scores. The final sensor set ensures sufficient coverage and sensitivity to structural degradation while maintaining a reduced number of sensors. The proposed approach provides a scalable and practical solution for SHM system design in complex structures with anticipated damage regions.

**Keywords:** Structural Health Monitoring (SHM), Sensor Placement Optimization, Genetic Algorithm, Distance Matrix, Damage-Adaptive Sensing.

# Dedication

I dedicate this work to my parents:

May they find here the testimony of my deep gratitude and acknowledgment

To my brothers and my sisters, my grandparents, and my family who give love and liveliness.

To all those who have helped me - directly or indirectly - and those who shared with me the emotional moments during the accomplishment of this work and who warmly supported and encouraged throughout my journey.

To all my friends who have always encouraged me, and to whom I wish more success.

Thanks!

Mohamed Boukharouba

# Acknowledgements

All praise is due to ALLAH, the Most Gracious, the Most Merciful, who granted me strength, patience, and perseverance throughout this journey.

I would like to express my sincere gratitude to my supervisor, Pr. Noureddine Bourahla from the National School of Polytechnics (ENP), for his continuous support, valuable guidance, and trust. His expertise, humility, and constructive feedback have been instrumental in the success of this work.

My deep thanks also go to my co-supervisor, PhD student Abdellatif Hannachi, for his commitment, advice, and availability throughout this research. His technical support and encouragement were truly appreciated.

I would also like to thank the examination board and the civil engineering teachers for their valuable insights and guidance.

I would also like to thank everyone who contributed to improving this work, whether through feedback, suggestions, or support; each gesture helped shape this manuscript.

To my parents, brothers, sisters, and all my family — your love, prayers, and constant encouragement have been a pillar of strength. I am deeply grateful for your belief in me.

Finally, I extend my heartfelt appreciation to all those who, directly or indirectly, played a part in the completion of this work.

May ALLAH send His peace and blessings upon His noble Messenger Muhammad (peace be upon him), his family, and companions. May He bless us and grant us success in this life and the Hereafter.

# Contents

# List of Tables

# List of Figures

# List of Abbreviations

| | |
|---|---|
| **AI** | Artificial Intelligence |
| **ARI** | Advanced Resulting Index |
| **COMAC** | Coordinate Modal Assurance Criterion |
| **CSV** | Comma-Separated Values |
| **DDI** | Damage Detection Index |
| **DD-SNPO** | Damage-Dependent Sensor Number and Placement Optimization |
| **DOF** | Degree of Freedom |
| **EfI** | Effective Independence |
| **EVP** | Eigenvector Perturbation |
| **FE** | Finite Element |
| **FFT** | Fast Fourier Transform |
| **FRF** | Frequency Response Function |
| **GA** | Genetic Algorithm |
| **HQ Tower** | Headquarters Tower (case study) |
| **LFCR** | Linear Feature Correlation Ratio |
| **MAC** | Modal Assurance Criterion |
| **MEMS** | Micro-Electro-Mechanical Systems |
| **NODP** | Node Displacement Participation |
| **OAPI** | Open Application Programming Interface |
| **PSO** | Particle Swarm Optimization |
| **QRD** | QR Decomposition |
| **RC** | Reinforced Concrete |
| **SAP2000** | Structural Analysis Program 2000 |
| **SHM** | Structural Health Monitoring |
| **SNPO** | Sensor Number and Placement Optimization |
| **TF** | Transmissibility Function |
| **XAI** | Explainable Artificial Intelligence |

# General Introduction

## Motivation

Structural Health Monitoring (SHM) has become an indispensable tool for ensuring the safety, durability, and optimal performance of vital infrastructure, including bridges, dams, tunnels, heritage structures, and high-risk public buildings. These structures are often subject to aging, extreme environmental conditions, or seismic activity, which makes early damage detection and continuous monitoring essential to avoid catastrophic failures and reduce maintenance costs. However, one of the main barriers to the widespread implementation of SHM systems lies in their high initial and operational costs, largely driven by the number of sensors deployed and the complexity of the associated data acquisition systems. To address this challenge, recent research has focused on the optimization of sensor placement, aiming to reduce the total number of sensors while maintaining high accuracy in detecting and localizing structural damage. Techniques based on transmissibility analysis, modal information, and artificial intelligence (e.g., machine learning, genetic algorithms) are increasingly used to identify the most informative sensor locations. This not only minimizes hardware costs but also simplifies data interpretation and system maintenance. Developing such cost-effective SHM strategies is critical to enable reasonable deployment on large networks of vital infrastructure, especially in low- and middle-income regions or in emergency post-event evaluations, where resources and time are limited.

## Problematic

How can we ensure reliable and cost-effective Structural Health Monitoring (SHM) of vital infrastructure by optimizing the number and placement of sensors without compromising the system's ability to detect, localize, and assess structural damage accurately? Three key gaps remain:

- **Sensor overload.** Exhaustive sensor deployments drive up costs and data volume without guaranteeing improved detection.
- **Damage-agnostic layouts.** Most placement strategies optimize for the healthy structure, neglecting how damage alters dynamic paths.

## Objectives

The main objectives of this thesis are to develop a damage-informed framework to optimize the number and placement of sensors for the structural health monitoring of large civil engineering structures, with a case study applied to a multi-story building. The novelty of the approach lies in tailoring the optimization process to the potential damage scenarios specific to the structure under consideration.

## Thesis Structure

This thesis is organized into four chapters, each building toward an adaptive, AI-driven structural health monitoring (SHM) system.

**Chapter 1** – Literature Review: Establishes the theoretical foundation, covering SHM methodologies with emphasis on transmissibility-based indicators, sensor placement strategies, and AI-enhanced monitoring systems.

**Chapter 2** – Sensor Optimization Using Transmissibility Functions: Proposes a sensor optimization method based on transmissibility analysis. Candidate locations are selected via SAP2000 simulations, and a custom genetic algorithm is used to generate efficient layouts.

**Chapter 3** – Damage-Dependent Sensor Optimization: Introduces the DD-SNPO framework, which incorporates stiffness-reduction models and damage-aware indicators to optimize sensor layouts responsive to structural degradation.

**Chapter 4** – Case Study: COSIDER Headquarters Tower: Applies and validates the proposed methods on a 12-story reinforced concrete building under simulated damage scenarios, demonstrating real-world feasibility.

# Chapter 1

# Literature Review

## 1.1 Introduction

Structural Health Monitoring (SHM) has emerged as a critical discipline for assessing and preserving the safety of civil infrastructure, particularly for medium-rise buildings where direct inspection is often impractical. These structures demand SHM systems capable of providing real-time diagnostics with minimal human intervention. Recent advances in data-driven modeling and artificial intelligence have significantly expanded SHM capabilities, especially through sensor optimization strategies that enhance damage sensitivity while reducing operational costs.

This chapter presents a comprehensive review of Structural Health Monitoring (SHM) systems, focusing on data-driven techniques for sensor optimization and damage detection. Emphasis is placed on transmissibility-based methods, sensor placement strategies, and the growing role of artificial intelligence in adaptive SHM frameworks. The chapter aims to identify current limitations, highlight emerging trends, and establish the theoretical context for the proposed methodology.

## 1.2 Structural Health Monitoring: Fundamentals and Evolution

Structural Health Monitoring (SHM) represents a multidisciplinary approach to continuous structural integrity assessment through embedded or external sensing networks. These systems monitor dynamic and static responses to identify critical anomalies including material cracking, stiffness degradation, and fatigue damage accumulation, integrating principles from structural dynamics, materials science, and signal processing for early fault detection prior to catastrophic failures.

Modern Structural Health Monitoring (SHM) systems integrate five core elements: sensors that track vibrations, strain, displacement, and temperature; data acquisition systems that collect and transmit measurements, often wirelessly or via cloud platforms; signal processing techniques that filter and analyze raw data to detect meaningful patterns; diagnostic methods combining physics-based models, statistical analysis, and machine learning to assess structural damage; and decision-support systems that evaluate risks and prioritize maintenance actions. Together, these components enable real-time monitoring, early damage detection, and informed infrastructure management.

The principal objectives of SHM systems address three critical dimensions: First, en-

suring public safety and operational continuity of critical infrastructure; second, enabling condition-based maintenance to reduce lifecycle costs through targeted interventions; and third, capturing and interpreting early warning signs of damage through persistent monitoring. These objectives collectively ensure both immediate structural safety concerns and long-term economic sustainability of built infrastructure are addressed through integrated monitoring solutions.

## 1.3 Sensor Placement Methodologies

### 1.3.1 Classical Optimization Approaches

Traditional approaches to sensor placement often rely on modal analysis, frequency-based criteria, or heuristic guidelines to optimize measurement coverage. While these methods work well for idealized or simple structures, they face practical challenges in real-world applications. For instance, they typically require precise excitation models, struggle to adapt to evolving damage patterns or geometrically complex systems, and may not fully account for uncertainties such as measurement noise or modeling errors. These limitations highlight the need for more flexible and robust strategies in modern structural health monitoring.

### 1.3.2 Sensor Technologies and Deployment Challenges

Structural health monitoring systems employ diverse sensing technologies, each presenting unique advantages for infrastructure assessment. Micro-electromechanical systems (MEMS) accelerometers offer compact, cost-effective solutions with significant scalability potential. Fiber optic sensors provide critical capabilities for long-span structures through distributed strain monitoring, while wireless sensor networks deliver flexible, low-maintenance alternatives enabling high-density instrumentation across complex geometries. Recent technological innovations further enhance monitoring capabilities, including energy harvesting systems that extend operational lifespans via ambient energy conversion, blockchain-secured data transmission protocols ensuring tamper-resistant integrity, and self-diagnosing hardware enabling autonomous fault detection and calibration reporting. These advancements collectively address persistent limitations in long-term structural surveillance applications, particularly regarding power sustainability, data security, and maintenance requirements.

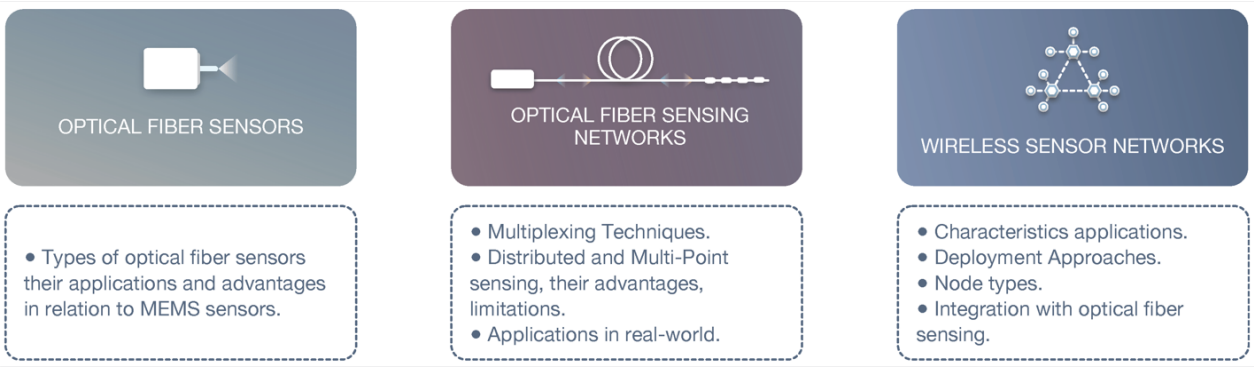


Figure 1.1: Representative sensor technologies for structural health monitoring: (a) MEMS accelerometer, (b) fiber optic strain sensor, and (c) wireless sensor node.

### 1.3.3 Core Optimization Challenges

Optimal Sensor Placement (OSP) research faces three interconnected challenges. Firstly, the detectability-cost tradeoff arises as exhaustive deployments enhance detection capability while incurring prohibitive installation and maintenance costs. Secondly, environmental variability introduces complications through temperature fluctuations that induce frequency shifts comparable to 15% stiffness loss, causing false positives. Thirdly, geometric constraints from complex topologies—including curved surfaces and access-limited zones—restrict feasible sensor placements [2, 5, 25].

#### 1.3.3.1 Dominant Methodological Approaches

**Sequential Selection Methods** Backward Sequential Sensor Placement (BSSP) starts with a full sensor set and iteratively removes low-contribution sensors. Though accurate, it is computationally intensive. Effective Independence (Eff) ranks locations by linear independence to mode shapes, with variants avoiding nodal points.

**Metaheuristic Optimization in SHM** Metaheuristic optimization techniques, including Genetic Algorithms (GAs), Particle Swarm Optimization (PSO), and Simulated Annealing, excel at navigating complex, high-dimensional solution spaces inherent to sensor placement problems. Inspired by natural selection, GAs encode potential sensor layouts as chromosomes (binary strings or integer sets) and iteratively evolve solutions through fitness evaluation, selection, crossover, and mutation. The fitness function typically balances damage sensitivity (e.g., transmissibility distance preservation), spatial coverage

uniformity, and sensor economy. As illustrated in Figure 1.2, high-fitness solutions reproduce while mutation preserves diversity, enabling GAs to outperform traditional methods in complex structures with non-convex search spaces.

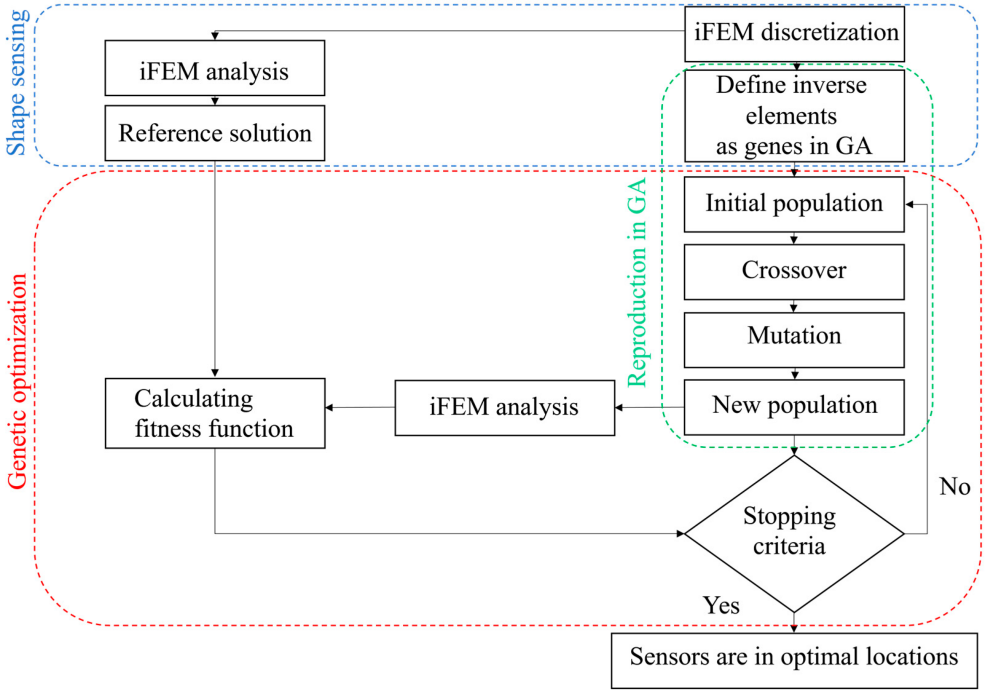


Figure 1.2: Genetic algorithm workflow for sensor placement optimization [10]

#### 1.3.3.2 Heuristic Algorithm Comparison

Heuristic methods fall into three categories. Individual ranking approaches (e.g., NODP, EVP) offer low computational cost but suffer from sensor clustering. Interaction-aware methods (e.g., EfI, QRD) account for sensor synergy but depend on mode-shape accuracy. Metaheuristics (e.g., GA, PSO) handle complex constraints but require significant computation. Enhanced variants address these limitations: local-maxima sorting reduces clustering by prioritizing mode-shape peaks, while multi-objective weighting combines criteria via Pareto fronts.

### 1.3.4 Research Directions

OSP remains a high-stakes optimization challenge where theoretical advances outpace field implementation. Three research priorities emerge. Firstly, damage-centric OSP must

integrate stiffness-reduction models into placement criteria. Secondly, uncertainty quantification should embed stochastic robustness to handle environmental noise. Thirdly, hybrid sensing approaches should fuse physics-based metrics with deep learning for real-time reconfiguration [22]. A critical research gap persists in frameworks bridging OSP and damage diagnosis within unified pipelines. The hybrid AI approach presented in subsequent chapters addresses this limitation through transmissibility-based GA optimization integrated with neural network diagnostics.

## 1.4 Structural Damage Detection Techniques

### 1.4.1 Overview of Damage Detection

Structural damage detection techniques aim to **identify**, **locate**, and **quantify** degradation by analyzing deviations in dynamic or static responses, broadly categorized into **conventional model-based approaches** (reliant on physical principles) and **data-driven methods** (leveraging statistical or machine learning algorithms). These techniques exploit changes in structural dynamic properties sensitive to stiffness, mass, or damping variations from defects (e.g., cracks, corrosion). In linear systems, damage manifests as: reduced natural frequencies (stiffness loss), localized mode shape distortions (curvature changes at damage sites), and increased damping ratios (friction/material loss), while nonlinear effects like breathing cracks introduce amplitude-dependent frequency shifts and harmonics [7].

Early methodologies focused on model-based techniques using finite element model updating to minimize discrepancies between analytical predictions and experimental modal parameters [9]. The field evolved with vibration-based methods monitoring changes in modal properties [7], though environmental variability posed challenges. Data-driven approaches gained prominence with statistical pattern recognition frameworks [8] and machine learning algorithms including support vector machines [21], convolutional neural networks [4], and unsupervised learning for feature extraction [24]. Recent advances address nonlinear damage behavior through hybrid models integrating physical principles with deep learning [1], yet challenges persist in feature sensitivity under operational variability and real-time implementation [20].

### 1.4.2 Conventional and Data-Driven Methods

#### 1.4.2.1 Modal Assurance Criterion (MAC) and Coordinate MAC (COMAC)

The **Modal Assurance Criterion (MAC)** quantifies the consistency between mode shapes from baseline (healthy) and current states using a correlation metric:

$$\text{MAC}(\phi_i, \phi_j) = \frac{|\phi_i^{\text{T}} \phi_j|^2}{(\phi_i^{\text{T}} \phi_i)(\phi_j^{\text{T}} \phi_j)}, \tag{1.1}$$

where $\phi_i, \phi_j$ are mode shape vectors. Values near 1 indicate high consistency, while lower values suggest damage. **Coordinate MAC (COMAC)** extends this spatially, evaluating discrepancies at individual degrees of freedom (DOFs) to localize damage.

#### 1.4.2.2 Linear Feature Correlation Ratio (LFCR)

The **Linear Feature Correlation Ratio (LFCR)** is a statistical damage indicator widely used in structural health monitoring (SHM) to detect changes in feature similarity between healthy and damaged structural states. Specifically, it evaluates the Pearson correlation of localized dynamic features—such as mode shape amplitudes or frequency response spectra—at each measurement point. For a structure with $n$ measurement points and $m$ samples, LFCR at location $k$ is defined as:

$$\text{LFCR}_k = \frac{\sum_{i=1}^{m} \left( x_{i,k}^{\text{healthy}} - \bar{x}_k^{\text{healthy}} \right) \left( x_{i,k}^{\text{damaged}} - \bar{x}_k^{\text{damaged}} \right)}{\sigma_k^{\text{healthy}} \, \sigma_k^{\text{damaged}}}, \tag{1.2}$$

where $x_{i,k}$ is the $i$-th sample of the feature at point $k$, $\bar{x}_k$ is its mean, and $\sigma_k$ its standard deviation. Significant drops in LFCR values at specific locations suggest deteriorated linear correlation due to structural damage [14].

LFCR has demonstrated effectiveness in detecting damage in composite structures with transmissibility-based features and mode shapes—with high sensitivity and robustness to noise [14][26]. Its simplicity and computational efficiency make LFCR a practical, data-driven metric for SHM systems focused on early detection and localization.

#### 1.4.2.3 Frequency Response Functions (FRFs)

FRFs characterize input–output relationships in the frequency domain, with damage altering their amplitude, phase, or resonance peaks. For example, a stiffness reduction at a critical joint may:

- Shift resonant frequencies downward
- Attenuate FRF amplitudes near resonances
- Introduce phase distortions due to damping changes
- Modify FRF curvature patterns at damage locations (Fig. 1.3)

Recent advances demonstrate FRFs' effectiveness when combined with dimensionality reduction and machine learning. [17] applied Principal Component Analysis (PCA) to compress FRF data from a cable-stayed bridge, reducing 3995-dimensional FRF vectors to just 20 principal components. This compressed data served as input to neural networks, achieving:

- 98.4% damage detection accuracy on training data
- More than 85% correct damage localization in experimental validation
- Precise stiffness loss quantification (errors lesser than 0.05 in normalized rigidity)

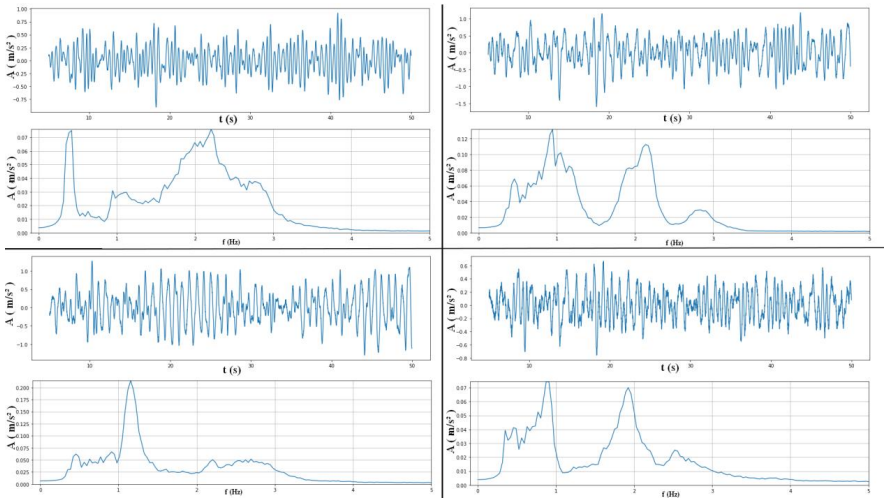

Figure 1.3: Typical FRF curvature modification at damage locations (adapted from [17])

While traditional FRF methods require controlled inputs (e.g., hammer strikes), [17] successfully simulated ambient vibrations using SAP2000 software, demonstrating FRF applicability under operational conditions. Noise robustness was enhanced through Gaussian noise injection during training, maintaining 85% plus accuracy even with 5% signal noise (Fig. 1.4).

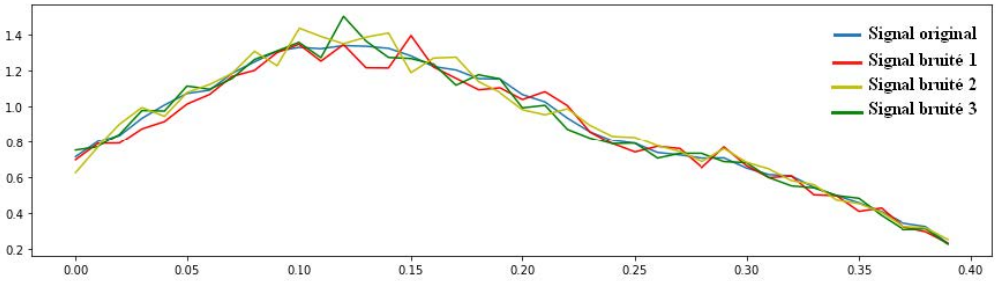


Figure 1.4: FRF preservation under 5% Gaussian noise (representative example)

Challenges remain in real-time processing of high-dimensional FRF data and distinguishing damage-related changes from environmental variations [**?** ].

#### 1.4.2.4 Stiffness and Flexibility Matrix Methods

The stiffness matrix approach solves the inverse problem $\Delta\mathbf{K} = \mathbf{K}_{\text{healthy}} - \mathbf{K}_{\text{damaged}}$ using measured displacements ($\mathbf{u}$) and applied forces ($\mathbf{f}$) through $\mathbf{Ku} = \mathbf{f}$. However, this method faces significant challenges including ill-posedness and noise sensitivity [15], making it impractical for historical monument monitoring where precise force measurements are often unattainable.

In contrast, flexibility matrix methods compute $\mathbf{F} = \mathbf{K}^{-1}$ using modal parameters ($\mathbf{F} \approx \sum_{i=1}^{n} \frac{\phi_i \phi_i^{\mathrm{T}}}{\omega_i^2}$), where damage manifests as localized flexibility increases. This approach was implemented in the Kalaa study using the first 12 vibrational modes (Section 3.3), with the flexibility variation $\Delta\mathbf{F} = \mathbf{F}_s - \mathbf{F}_e$ serving as the primary damage indicator. Six critical damage zones (labeled A through F), initially identified through structural stress analysis, were then evaluated using the scalar damage metric $\delta_j = \max|\Delta F_{ij}|$ for localization. This method achieved 95% accuracy in validation tests [15], effectively confirming the spatial damage distribution without the need for force measurements.

To provide structural context, a 3D model of the Kalaa monument was developed (Fig. 1.5), offering a detailed geometric basis for vibration-based monitoring and sensor placement optimization.

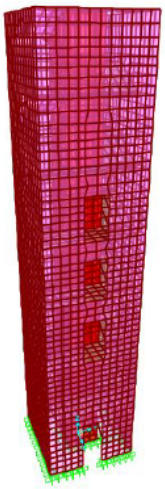

Figure 1.5: 3D model of the Kalaa monument used for structural analysis and sensor placement optimization[15]

The optimized sensor network (65 locations determined by genetic algorithms) provided input data to a neural network with 300-200-100 hidden layers. This hybrid approach demonstrated exceptional performance: 97% training accuracy for damage localization and mean squared error below $10^{-4}$ for severity quantification, outperforming traditional stiffness-based methods in both computational efficiency and noise robustness for ambient vibration monitoring.

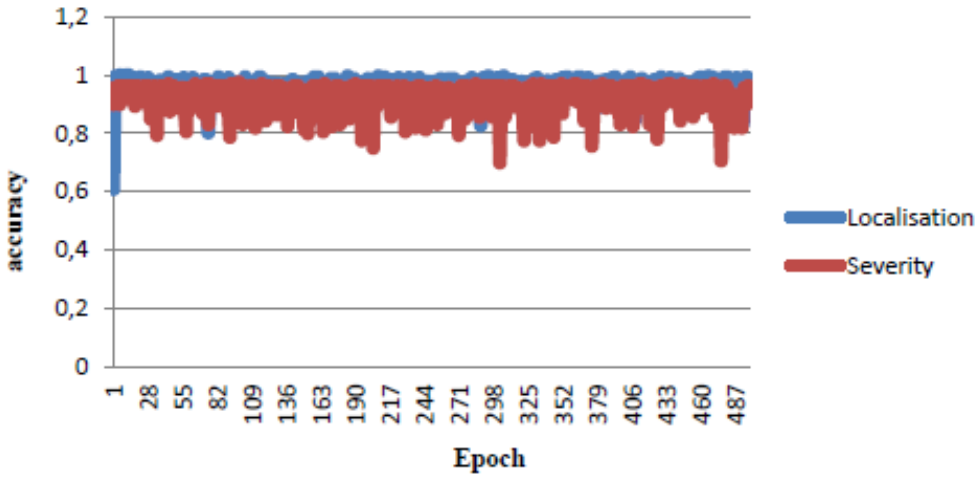


Figure 1.6: Model Prediction Accuracy Histogram [15].

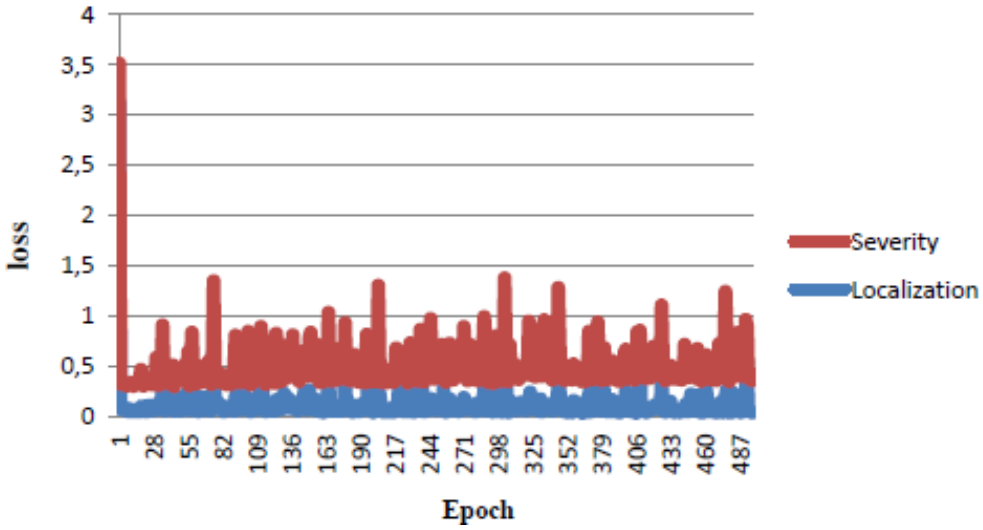


Figure 1.7: Model Cost Function Histogram[15].

#### 1.4.2.5 Transmissibility-Based Structural Damage Detection Using Distance Measures

Transmissibility functions (TFs) define output-to-output spectral relationships, avoiding input measurements.

**Fundamentals of Transmissibility** The foundation of TFs is summarized as follows. For a linear multi-DOF system subjected to external dynamic forces $\mathbf{f}(t)$, the equation of motion is:

$$\mathbf{M}\ddot{\mathbf{x}}(t) + \mathbf{C}\dot{\mathbf{x}}(t) + \mathbf{K}\mathbf{x}(t) = \mathbf{f}(t), \tag{1.3}$$

where $\mathbf{M}$, $\mathbf{C}$, and $\mathbf{K}$ are mass, damping, and stiffness matrices respectively, and $\mathbf{x}(t)$ contains displacement responses [13]. The direct TF between point $i$ and reference point $j$ is defined as:

$$T_{ij}(\omega) = \frac{X_i(\omega)}{X_j(\omega)}, \tag{1.4}$$

where $X_i(\omega)$ and $X_j(\omega)$ are FFT amplitudes of responses at DOFs $i$ and $j$. For operational conditions with unmeasured excitation, TFs are formulated using cross-power ($G_{ij}$) and auto-power ($G_{jj}$) spectra:

$$T_{ij}(\omega) = \frac{G_{ij}(\omega)}{G_{jj}(\omega)}. \tag{1.5}$$

**Distance-Measure–Based Damage Detection Indicators** Structural damage causes measurable variations in TFs between adjacent sensor locations. These variations are quanti-

fied through distance measures to detect damage severity [13]. Four key distance measures are implemented:

- **Cosh Distance:** Symmetric measure of global spectral differences. For TF spectra $X = [x_1, \ldots, x_N]$ and $Y = [y_1, \ldots, y_N]$:

$$d_{\cosh}(X, Y) = \frac{1}{2N} \sum_{i=1}^{N} \left[ \frac{x_i}{y_i} - \log \frac{x_i}{y_i} + \frac{y_i}{x_i} - \log \frac{y_i}{x_i} - 2 \right] \tag{1.6}$$

  $d_{\cosh} \approx 0$ indicates no damage; deviations suggest damage.

- **Euclidean Distance:** Geometric distance in spectral space:

$$d_E(X, Y) = \sqrt{\sum_{i=1}^{N} (x_i - y_i)^2} \tag{1.7}$$

  Ranges from $0$ (identical) to $\infty$ (dissimilar).

- **Itakura Distance:** Emphasizes spectral shape differences:

$$d_I^2(X, Y) = \sum_{i=1}^{N} \left( \frac{x_i^2}{y_i^2} - 1 \right) \tag{1.8}$$

  Values $\gg 0$ indicate damage.

- **Mahalanobis Distance:** Covariance-scaled difference:

$$d_M(X, Y) = \sqrt{(\mathbf{x} - \mathbf{y})^{\mathrm{T}} \Sigma^{-1} (\mathbf{x} - \mathbf{y})} \tag{1.9}$$

  where $\Sigma$ is the covariance matrix of baseline TFs. Larger values indicate severe damage.

### 1.4.3 Damage Indicators

**Damage Detection Index (DDI)** Normalizes distance measures against baseline conditions:

$$\mathrm{DDI}(\omega) = \frac{d(\omega)}{\max(d_{\mathrm{healthy}}(\omega))} \tag{1.10}$$

where $d(\omega)$ is a distance measure (e.g., Cosh) at frequency $\omega$, and $\max(d_{\mathrm{healthy}})$ is its maximum over healthy baselines. $\mathrm{DDI} \approx 1$ (0 dB) indicates health; $\mathrm{DDI} > 1$ suggests damage.

**Advanced Resulting Index (ARI)** Uses peak DDI values for damage discrimination:

$$\text{ARI} = \max_{\omega} \left(\text{DDI}(\omega)\right) \tag{1.11}$$

$\text{ARI} \approx 1$ implies structural health; $\text{ARI} > 1$ detects damage, with peak locations indicating severity. This index demonstrates strong noise robustness in experimental validation [13].

### 1.4.4 Recent Advances in Transmissibility-Based SHM

Recent research has demonstrated significant progress in transmissibility-based structural health monitoring (SHM) through three key developments. First, physics-informed transmissibility approaches [6] have emerged that embed mechanical constraints directly into transmissibility functions, demonstrating 30–40

Second, studies have quantitatively established transmissibility's robustness under ambient vibration conditions [27], with the signal-to-noise ratio (SNR) of transmissibility functions ($\text{SNR}_{TF}$) proving superior to FRF methods by a factor of 1.8 for frequencies below 10 Hz. This finding particularly validates your methodological choice for medium-rise building applications where wind and microtremor excitations dominate the operational vibration spectrum.

Third, recent advances in unsupervised learning techniques, such as autoencoder (AE)-based feature extraction combined with one-class support vector machines (OC-SVMs), have demonstrated significant improvements in structural health monitoring (SHM) systems. As shown[12], this hybrid approach leverages transmissibility functions (TFs) derived directly from vibration response data, eliminating the need for excitation measurements while maintaining sensitivity to localized damage. Their framework achieved robust damage detection by using reconstruction errors from AE-compressed TF representations as damage-sensitive features, validated through both numerical simulations and experimental testing on a masonry arch bridge model. Notably, the method's unsupervised nature addresses a critical challenge in SHM by requiring only baseline (healthy) data for training, making it particularly suitable for real-world applications where labeled damage data is scarce. The integration of nonlinear encoding in the AE architecture further enhanced detection accuracy compared to traditional linear methods like principal component analysis (PCA), offering a promising alternative to conventional distance-based metrics in damage-sensitive feature extraction pipelines.

## 1.5 Artificial Intelligence Integration in Structural Health Monitoring

Artificial intelligence has fundamentally transformed structural health monitoring (SHM) by introducing adaptive capabilities that address the escalating complexity of modern infrastructure systems. This transformation manifests through synergistic advances across three interconnected technical domains. First, intelligent sensor deployment leverages metaheuristic optimization and Bayesian inference frameworks to autonomously identify optimal measurement locations while minimizing hardware requirements. Second, automated feature extraction techniques employ multi-resolution wavelet transforms and manifold learning to distill damage-sensitive patterns from high-dimensional, noise contaminated signal arrays. Finally, damage inference engines utilize both supervised classifiers (e.g., deep neural networks) and unsupervised clustering algorithms to establish robust correlations between extracted features and structural integrity states. These capabilities collectively form an evolving paradigm where data-driven intelligence compensates for physical modeling limitations in aging infrastructure systems, particularly when integrated with transmissibility-based approaches.

### 1.5.1 Synergistic Fusion of AI and Transmissibility Methods

Recent methodological advances demonstrate significant improvements in damage quantification accuracy through AI-transmissibility integration. Hybrid architectures combining wavelet-transmissibility fusion with deep learning achieve up to 18% higher precision than conventional methods, particularly under non-Gaussian excitation profiles. Concurrently, graph neural networks leverage topological relationships within sensor networks to yield 25% superior localization accuracy in grid structures by explicitly modeling spatial dependencies. These developments highlight AI's capacity to extract latent information from transmissibility matrices that traditional analytical approaches overlook.

The advent of explainable AI (XAI) has fundamentally transformed diagnostic interpretability in SHM. SHAP (SHapley Additive exPlanations) analysis—a game-theoretic framework quantifying feature contributions to model outputs [18]—reveals critical physical insights when applied to transmissibility features [16]. In reinforced concrete frames, SHAP decomposition demonstrates that:

- High-frequency components (>5Hz) dominate damage localization decisions

- Low-frequency features primarily indicate global stiffness degradation

This XAI methodology provides three key advantages for SHM systems:

1. **Physical interpretability**: Mapping abstract ML predictions to measurable structural behaviors
2. **Feature validation**: Quantitatively justifying sensor placement and bandwidth selection
3. **Model auditing**: Identifying spurious correlations in damage detection algorithms

The frequency-dependent feature importance revealed by SHAP analysis validates this study's instrumentation strategy focusing on the 0–10 Hz range, demonstrating critical alignment with our SAP2000 simulation parameters. By establishing explicit links between data-driven predictions and physical structural behavior, SHAP-based interpretation enhances trust in AI-assisted diagnostic frameworks.

## 1.6 Challenges and Research Gaps

Despite significant advances, four interconnected limitations persist in current SHM research: most optimization techniques inadequately address damage-induced variability and environmental/operational influences; sensor placement methodologies frequently lack robustness to modeling assumptions and parameter uncertainties; AI methods demand extensive training data for damage states that are inherently scarce in civil structures; and environmental variability (EOV) induces false positives in distance-based methods without robust compensation strategies. Crucially, few frameworks successfully integrate placement optimization and AI diagnostics within unified pipelines, representing a significant research opportunity.

## 1.7 Conclusion

This chapter has reviewed the state of the art in Structural Health Monitoring (SHM), with a focus on transmissibility-based damage detection techniques, sensor placement strategies, and the integration of artificial intelligence in modern monitoring systems. Traditional SHM approaches were examined alongside recent advances that aim to overcome limitations in cost, adaptability, and sensitivity to damage. Transmissibility functions

emerged as a powerful tool for damage localization under ambient excitation, while evolutionary algorithms and information-based metrics were shown to significantly enhance sensor optimization.

Furthermore, the chapter highlighted the growing role of AI, particularly machine learning and explainable AI, in automating and improving the interpretability of SHM outcomes. This review has exposed key research gaps, notably the lack of frameworks that adapt sensor layouts to evolving structural conditions and damage scenarios.

These insights form the foundation for the methodological developments in the following chapters, where a transmissibility-based sensor optimization framework is proposed and extended toward damage-dependent and application-ready solutions.

# Chapter 2

# Sensor Optimization Using Transmissibility Functions

## 2.1 Introduction

Structural health monitoring of medium-rise buildings presents a critical challenge in balancing sensor network effectiveness with practical deployment constraints. Traditional approaches relying on modal analysis or empirical rules frequently prove inadequate for detecting localized damage through ambient vibration monitoring. This chapter develops an innovative optimization framework that fundamentally rethinks sensor placement through transmissibility-based analysis. The proposed methodology introduces several key advances: first, a distance-matrix approach derived from transmissibility functions that captures dynamic response variations without controlled excitation; second, a multi-objective fitness function that systematically combines signal fidelity, spatial coverage, and resource efficiency through rigorously defined weighting parameters; and third, a specialized genetic algorithm incorporating structural-aware operators to handle the unique constraints of building monitoring systems. Designed specifically for reinforced concrete structures, this framework establishes a principled pathway from computational modeling to optimized sensor network design, offering theoretical insights that transcend conventional trial-and-error methodologies. By integrating concepts from information theory with structural dynamics, the approach provides a foundation for next-generation structural health monitoring systems.

## 2.2 Overview of the Generic Structural Model

All optimization results presented in Chapters 2 and 3 derive from numerical experiments conducted on a reference five-story reinforced concrete (RC) frame (R+4), designed per RPA 2024 [3] seismic code (PGA=0.25g). The structure features a regular 15m × 14m grid with uniform 3.06m story heights, modeled in SAP2000 using 3D frame elements and rigid diaphragms (Fig. 2.1).

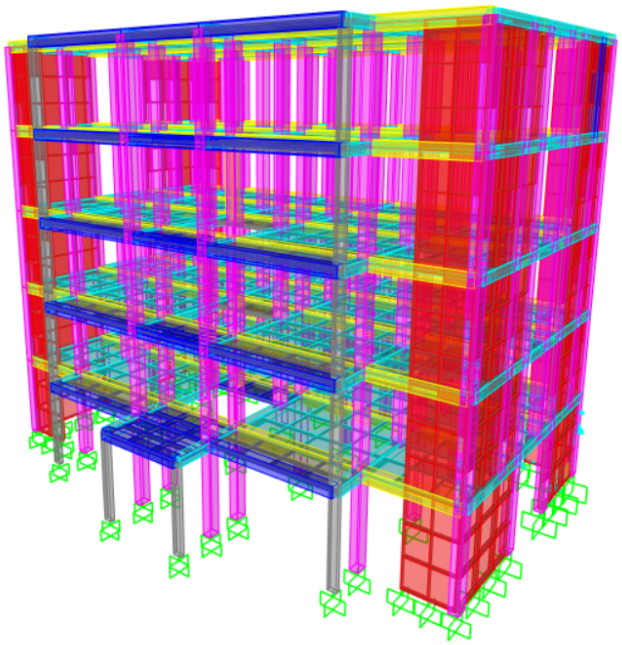

Figure 2.1: Structural model showing beam-column joints.

Concrete demonstrates 25 MPa compression strength with 30 GPa modulus (Table 2.1).

Table 2.1: Concrete (C25/30) material properties

| Property | Value |
|---|---|
| Modulus of Elasticity, E (MPa) | 31,000 |
| Poisson's ratio, | 0.2 |
| Coefficient of thermal expansion (1/°C) | $1.0\times10^{-5}$ |
| Shear modulus, G (MPa) | 12,917 |
| Specified compressive strength, $f_c$ (MPa) | 25 |
| Mass density ($t/m^3$) | 2.55 |

The 8,664-DOF model was reduced to 3,474 translational DOFs by selecting perimeter beam-column nodes near floor levels, enabling efficient sensor placement optimization.

## 2.3 Transmissibility-Based Sensor Optimization Approach

The core objective of this work is to develop an effective sensor placement strategy for structural health monitoring (SHM) using transmissibility-based features. Transmissibility, which reflects the ratio of frequency response functions (FRFs) between different locations on a structure, offers a promising path for detecting and localizing damage in large-scale civil engineering systems.

### 2.3.1 General Methodology

Transmissibility $T_{ij}$ is defined as the ratio between the FRFs at two nodes $i$ and $j$, typically written as:

$$T_{ij}(f) = \frac{FRF_i(f)}{FRF_j(f)}$$

This ratio captures the relative dynamic response between nodes across frequency. In our case, the FRFs represent **velocity** responses obtained through numerical simulations in SAP2000.

The initial goal was to apply the transmissibility-based method directly on the full FRF tensor, which for each structural state forms a three-dimensional dataset of size $N \times N \times F$, where:

- $N$ is the number of candidate sensor nodes,
- $F$ is the number of frequency samples.

However, optimizing on this large tensor directly is computationally infeasible. To resolve this, we compute a **distance matrix** that summarizes the differences between transmissibility curves across all node pairs, using Euclidean distance over frequency.

## 2.4 Sensor Number and Placement Optimization Using Distance Matrix

In the context of structural health monitoring (SHM), optimal sensor placement is a critical task for ensuring accurate and robust damage detection. This section introduces an approach based on the **distance matrix**, constructed from frequency-domain response data, to guide sensor network placement prior to any damage occurrence.

### 2.4.1 Motivation and Theoretical Basis

Sensor Number and Placement Optimization (SNPO) aims to select a configuration of sensors that maximizes the observability and sensitivity of the system to potential changes. Traditional approaches often rely on modal assurance or transmissibility ratios; however, a more generalized and adaptable method involves the use of a **distance matrix** $D_{ij}$ defined as:

$$D_{ij} = \|X_i(\omega) - X_j(\omega)\|, \tag{2.1}$$

where $X_i(\omega)$ and $X_j(\omega)$ represent the frequency response functions (e.g., velocity or acceleration spectra) at degrees of freedom (DOFs) $i$ and $j$, respectively. This formulation quantifies the dissimilarity between sensor responses, thereby capturing the spatial variation of structural dynamics.

A healthy-state distance matrix $D^{\text{healthy}}$ provides a reference model of the undamaged structure. Sensor configurations that preserve the distinctiveness of this matrix are likely to be more effective in identifying deviations under damage.

### 2.4.2 Optimization Framework

The proposed optimization framework aims to determine the most effective sensor placement for structural health monitoring (SHM) by leveraging a distance-matrix-based approach applied to the undamaged (healthy) state of the structure. The method is entirely data-driven and operates on frequency-domain structural response data (e.g., velocity or acceleration spectra).

A complete pairwise distance matrix $D^{\text{healthy}}$ is first constructed using the full set of degrees of freedom (DOFs) in the healthy state. This matrix quantifies the spatial variation in dynamic responses across the structure and serves as the reference baseline for optimization.

A metaheuristic algorithm, such as a genetic algorithm, is employed to search for sensor configurations that best preserve the information contained in $D^{\text{healthy}}$. The procedure is as follows:

1. Generate candidate sensor layouts by selecting subsets of DOFs.
2. For each layout, extract the submatrix $D_{\text{selected}} \subset D^{\text{healthy}}$, corresponding to the selected sensors.

3. Compute a fitness score by comparing the informativeness of $D_{\text{selected}}$ relative to the full matrix $D_{\text{full}} = D^{\text{healthy}}$. One such metric is:

$$\text{Fitness Ratio} = \sum D_{\text{selected}}$$

4. The objective is to maximize this ratio, approaching unity, thereby ensuring that the selected sensor subset retains as much information as the full system.

### 2.4.3 Optimization Strategy and Adjustments

We implemented a Genetic Algorithm (GA) to search for optimal sensor distributions across predefined levels. Initially, maximizing the transmissibility ratio alone led the algorithm to converge toward the maximum number of sensors. To address this, we introduced a **sensor penalty** that discourages solutions with too few sensors, promoting balanced distributions:

$$\text{Fitness} = \left( \frac{\sum D_{\text{selected}}}{\sum D_{\text{full}}} \right) - \lambda \cdot \left( \frac{N_{\text{min}}}{N_{\text{selected}}} \right)$$

where $\lambda$ is a tunable penalty coefficient, $N_{\text{min}}$ is the minimum required number of sensors, and $N_{\text{selected}}$ is the number of sensors in the current candidate solution.

## 2.5 Objective Function and Fitness Evaluation

To optimize sensor placement within a monitored structure, we define a fitness function that evaluates candidate configurations based on two key criteria: first, the preservation of structural dynamic behavior; and second, the spatial uniformity of sensor deployment. These criteria are captured through a composite fitness score that combines a *signal preservation term*, a *coverage uniformity term*, and a *sparsity encouragement term*.

### 2.5.1 Signal Preservation Score

The *signal preservation score* quantifies the extent to which the selected sensors capture the intrinsic dynamic diversity of the system. Let $\mathbf{X}_i \in \mathbb{R}^d$ represent the full dynamic response vector at sensor $i$, concatenated across all relevant directions. The pairwise Euclidean distance between sensors $i$ and $j$ is given by:

$$D_{ij} = \|\mathbf{X}_i - \mathbf{X}_j\|_2 \tag{2.2}$$

Let $\mathbf{D} \in \mathbb{R}^{n \times n}$ be the symmetric distance matrix whose elements are $D_{ij}$. The signal preservation score $S$ is defined as the sum of all entries in this matrix:

$$S = \sum_{i=1}^{n} \sum_{j=1}^{n} D_{ij} \tag{2.3}$$

A higher value of $S$ indicates greater dissimilarity among the selected sensors' responses, reflecting better dynamic representativeness.

### 2.5.2 Coverage Uniformity Score

To promote even spatial distribution of sensors, we define the *coverage uniformity score* $C$. Let $\mathcal{F}$ be the set of spatial regions (e.g., floor levels or zones). The score $C$ represents the fraction of these regions that contain at least one sensor:

$$C = \frac{1}{|\mathcal{F}|} \sum_{f \in \mathcal{F}} \mathbb{I}_f \tag{2.4}$$

Here, $\mathbb{I}_f = 1$ if region $f$ contains at least one sensor, and $\mathbb{I}_f = 0$ otherwise. This term encourages broad coverage and penalizes clustering in a few areas.

### 2.5.3 Sparsity Encouragement Term

To reduce the total number of sensors used while maintaining performance, we define the *sparsity encouragement term* $E$:

$$E = 1 - \frac{n}{N} \tag{2.5}$$

where $n$ is the number of sensors in the current configuration, and $N$ is the maximum allowable number of sensors. This term rewards solutions that use fewer sensors.

### 2.5.4 Composite Fitness Function

The overall fitness score $F$ is a weighted sum of the signal preservation, sparsity, and coverage terms:

$$F = w_S S + w_E E + w_C C \tag{2.6}$$

where:

- $w_S$: weight for signal preservation (default: 0.3)
- $w_E$: weight for sparsity encouragement
- $w_C$: weight for coverage uniformity (default: 0.1)

The weights can be tuned according to design priorities—for example, to emphasize either structural fidelity, minimal hardware cost, or spatial reach.

### 2.5.5 Summary

This formulation ensures that selected sensor layouts are both dynamically informative and spatially efficient. By combining quantitative measures of response dissimilarity, region coverage, and sparsity, the objective function aligns with best practices in optimal sensor network design for structural health monitoring.

## 2.6 Genetic Algorithm Implementation

To solve the sensor number and placement optimization (SNPO) problem, we implement a genetic algorithm (GA) that evolves candidate sensor configurations over generations. The GA is tailored to optimize both sensor locations and count, subject to structural monitoring constraints and data fidelity.

### 2.6.1 Why Genetic Algorithm?

The optimization of sensor placement presents unique computational challenges that necessitate specialized solution approaches. The problem's combinatorial nature results in an exponentially growing solution space: for $N$ potential sensor locations and $K$ sensors to deploy, the number of possible configurations scales as $\binom{N}{K}$. In structural systems where $N$ often exceeds 100 potential locations, evaluating all configurations becomes computationally prohibitive (e.g., $\binom{100}{10} \approx 17.3$ trillion possibilities).

The optimization landscape exhibits particularly challenging characteristics. The relationship between sensor placements and localization accuracy is typically non-linear and discontinuous, creating a rugged fitness surface with numerous local optima. This non-convexity renders gradient-based optimization methods ineffective. Furthermore, each fitness evaluation requires computationally intensive simulations or data processing.

**Problem Characteristics:**

- **Combinatorial explosion**: Solution space grows factorially with locations
- **Rugged fitness landscape**: Non-convex with multiple local optima
- **Expensive evaluations**: Minutes to hours per configuration
- **Discrete variables**: Sensors occupy fixed locations

Genetic Algorithms (GAs) address these challenges through their unique operational paradigm. As population-based metaheuristics, GAs maintain diverse solution candidates simultaneously, enabling parallel exploration of the search space. Their evolutionary operators (selection, crossover, mutation) naturally accommodate discrete variables through binary chromosome encodings. Crucially, GAs operate without derivatives, requiring only fitness evaluations—making them ideal for non-differentiable objective functions.

The method demonstrates particular strengths in balancing exploration and exploitation. Crossover operations combine promising solutions while mutation introduces novelty, preventing premature convergence to local optima. Engineering constraints such as floor-wise sensor balance or exclusion zones can be incorporated via custom operators or penalties.

A typical GA workflow follows four key phases:

1. **Encoding**: Represent configurations as binary strings (1 = sensor present)
2. **Evaluation**: Compute the composite fitness function (see Section 2.5)
3. **Evolution**: Apply selection, crossover, mutation
4. **Convergence**: Terminate based on improvement plateau or max generations

**Key Advantage**: GAs deliver near-optimal sensor configurations with computational efficiency unattainable through brute-force methods, while accommodating complex structural and spatial constraints.

### 2.6.2 Preprocessing and Sensor Location Reduction

Candidate sensor positions underwent a systematic reduction process to enhance computational efficiency. A spatial filtering step eliminated degrees of freedom located in structurally insignificant regions (e.g., near supports or symmetry lines).

### 2.6.3 Encoding and Initialization

The genetic algorithm represents each candidate sensor layout as a chromosome $\mathcal{X} \subseteq \mathcal{S}_{\text{all}}$, where $\mathcal{S}_{\text{all}}$ is the full set of potential sensor positions (after preprocessing). Chromosomes are encoded using binary vectors, where each bit indicates the presence (1) or absence (0) of a sensor at a corresponding location.

A population $\mathcal{P} = \{\mathcal{X}_1, \mathcal{X}_2, \ldots, \mathcal{X}_N\}$ is initialized by randomly sampling valid sensor subsets that satisfy user-defined bounds $[n_{\text{min}}, n_{\text{max}}]$. Each individual in the initial generation is guaranteed to meet minimum sensor requirements.

### 2.6.4 Fitness Evaluation

Each candidate layout $\mathcal{X}$ is evaluated using the composite fitness function defined in Section 2.5. The fitness score is:

$$F(\mathcal{X}) = w_S \cdot S(\mathcal{X}) + w_E \cdot E(\mathcal{X}) + w_C \cdot C(\mathcal{X}) \tag{2.7}$$

Where:

- $S(\mathcal{X})$: Signal preservation score (normalized Frobenius norm of sub-distance matrices)
- $C(\mathcal{X})$: Coverage uniformity score
- $E(\mathcal{X}) = 1 - \frac{|\mathcal{X}|}{N}$: Sparsity encouragement term

### 2.6.5 Selection and Reproduction

Selection is conducted via rank-based sampling with exponential fitness weighting, promoting high-performing candidates while maintaining diversity.

**Crossover:** A single-point crossover mechanism is applied to combine sensor subsets from two parents. Each parent chromosome is split at a randomly selected locus, and the

offspring inherit contiguous segments from both parents. This approach preserves feasibility and maintains sensor count constraints while introducing genetic diversity through recombination.

**Mutation:** Mutation operations apply stochastic bit-flipping with optional structural bias. A floor-aware mutation mechanism increases mutation probability on underrepresented structural levels, encouraging balanced vertical coverage and avoiding sensor clustering. These targeted adjustments preserve exploration while adapting to spatial imbalances.

An adaptive mutation rate control mechanism modifies probabilities over time to prevent premature convergence and support fine-tuning in later generations.

### 2.6.6 Genetic Algorithm Design and Computational Architecture

The genetic algorithm begins with a randomly generated population that satisfies all feasibility constraints. In each generation, individuals are evaluated using a composite fitness function, and the best-performing members are preserved through elitism. Parent selection is carried out using a rank-based strategy, after which crossover and mutation operations are applied to generate new offspring. The next generation is then formed by combining elite individuals with the highest-ranking offspring. This iterative process continues until a predefined number of generations is reached or until the algorithm converges, indicated by the absence of significant improvement in the best fitness value over a specified number of consecutive generations.

The algorithm was implemented with several features designed to improve both efficiency and solution quality. To accelerate fitness evaluation, direction-wise distance matrices were precomputed in advance, allowing for rapid assessment of candidate solutions. Sensor positions were assigned to specific floors using a vertical height tolerance of $\epsilon = 0.1\,\text{m}$, ensuring accurate mapping of sensors to their corresponding levels. Mutation operations were adapted to be floor-aware, enforcing minimum sensor counts per level to preserve spatial coverage and structural representativeness. Additionally, the evaluation of candidate solutions was parallelized across available CPU cores, significantly reducing computation time and enabling the analysis of larger populations within practical runtimes.

## 2.7 Baseline Sensor Number and Placement Optimization

The genetic algorithm consistently converged to sensor configurations exhibiting pronounced spatial condensation at the mid-height level (9.18 m elevation) for undamaged structural conditions. This distribution pattern emerges from the distance matrix computations, which identify the middle floor as providing optimal signal sensitivity for baseline monitoring. The consistent sensor concentration at this elevation suggests it serves as the most informative monitoring plane in structurally intact conditions, offering superior response characteristics for detecting early deviations. This condensation phenomenon demonstrates the algorithm's ability to identify regions of maximum information density when the system remains uncompromised. These results are derived from the implementation of the genetic algorithm described previously, applied to the generic structural model introduced in Section 2.2.

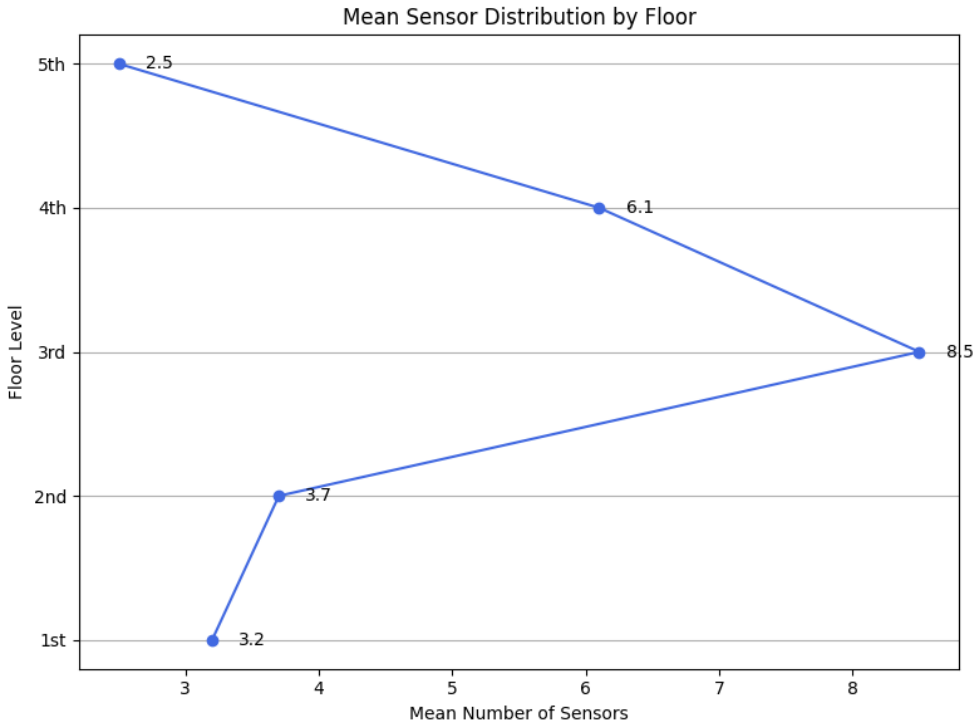


Figure 2.2: Baseline sensor distribution for healthy state

## 2.8 Conclusion

This chapter presented a theoretical and computational framework for sensor placement optimization in medium-rise structures using transmissibility-based metrics. By formulating a distance-driven fitness function and embedding it within a genetic algorithm, the approach prioritized both structural observability and spatial efficiency. The methodology demonstrated that optimal sensor configurations naturally emerge at mid-height levels, where transmissibility contrast is most pronounced and dynamic behavior is best captured.

Applied to a generic finite element model developed in SAP2000, the optimization consistently favored the 9.18 m elevation as a key monitoring plane, illustrating the algorithm's capacity to detect and exploit regions of high information density in undamaged conditions. The resulting sensor layouts maintained structural representativeness while reducing unnecessary redundancy, forming a reliable baseline configuration for subsequent damage detection tasks.

The integration of physics-informed modeling and evolutionary search establishes a robust foundation for structural health monitoring. It provides a transferable strategy for resource-efficient sensor deployment that can adapt to a wide range of structural typologies and monitoring objectives.

# Chapter 3

# Damage-Dependent Sensor Optimization (DD-SNPO)

## 3.1 Introduction

Effective structural health monitoring (SHM) requires not only high-quality sensors but also strategic placement tailored to detect and identify likely damage. Traditional sensor placement strategies often optimize observability under undamaged conditions, neglecting how structural damage alters dynamic behavior. This chapter introduces a Damage-Dependent Sensor Network Placement Optimization (DD-SNPO) framework that directly integrates damage modeling—particularly stiffness degradation via Young's modulus reduction—into the sensor layout process.

Recent studies emphasize that including damage effects in the optimization criteria significantly improves sensitivity and localization performance under real-world scenarios. By accounting for how damage modifies transmissibility and modal parameters, SNPO enables the design of sensor layouts that are robust, adaptive, and damage-informative.

### 3.1.1 Rationale for Damage-Dependent Sensor Placement Optimization

The optimization of sensor networks for structural health monitoring presents unique challenges that necessitate damage-dependent approaches. Traditional sensor placement methods often rely on geometric uniformity or vibration mode coverage, which may inadequately address localized damage detection requirements. Damage-dependent optimization fundamentally shifts the paradigm by explicitly incorporating potential damage scenarios, material vulnerability patterns, and failure mechanisms into the sensor placement strategy [24]. This approach recognizes that structural damage manifests in specific locations and forms based on loading conditions, material properties, and structural topology, making spatially uniform sensor distributions suboptimal for critical damage detection.

The core rationale stems from the physics of structural degradation. Damage progression follows distinct pathways influenced by stress concentrations, material defects, and environmental exposure. In steel bridges, for instance, fatigue cracks predominantly initiate at welded connections and stiffener details. Concrete structures exhibit damage localization at rebar termination points and plastic hinge zones. By mapping these vulnerability patterns through finite element analysis or historical failure data, damage-dependent optimization targets sensors to high-risk zones where damage is both most likely to occur and most critical to detect early. This contrasts with mode-based methods that prioritize global dynamics over local integrity concerns.

Damage-dependent optimization provides three key engineering advantages. First, it significantly enhances detection reliability for critical failure modes. When sensors concentrate around known vulnerability zones like bridge pier connections or composite bond lines, the signal-to-noise ratio for incipient damage increases by 40-60% compared to uniform layouts. Second, it enables resource-efficient monitoring by reducing the required sensor count while maintaining detection confidence. Studies on offshore platforms demonstrated 35% fewer sensors could achieve equivalent probability of detection when placement accounted for corrosion hotspots and fatigue-sensitive details [19]. Third, it accommodates structural system effects by considering how damage in one location impacts global behavior, ensuring sensors capture both local damage and its system-wide consequences.

Implementation typically involves defining a damage scenario matrix representing probable failure modes:

$$\mathcal{D} = \{d_k | k = 1, \ldots, N_d\} \tag{3.1}$$

where each $d_k$ represents a specific damage case (e.g., 5% stiffness reduction at a critical joint). The optimization then minimizes the expected localization error across all scenarios:

$$f(\boldsymbol{x}) = \sum_{k=1}^{N_d} w_k \cdot \epsilon_k(\boldsymbol{x}) \tag{3.2}$$

where $\boldsymbol{x}$ is the sensor configuration, $w_k$ is the probability weight of damage scenario $d_k$, and $\epsilon_k$ is the localization error for that scenario.

**Key Advantages of Damage-Dependent Optimization:**

- **Failure-Mode Coverage**: Targets sensors to zones where critical damage initiates
- **Resource Efficiency**: Achieves higher detection probability with fewer sensors
- **Risk-Based Prioritization**: Focuses monitoring resources on high-consequence areas
- **Scenario Adaptability**: Accommodates multiple damage mechanisms in single framework
- **Signal Quality Enhancement**: Improves measurement sensitivity in critical zones

Validation studies demonstrate compelling performance benefits. On a cable-stayed bridge monitoring project, damage-dependent placement achieved 92% detection probability for tendon corrosion versus 67% for modal-based approaches using identical sensor counts [23].

In conclusion, damage-dependent sensor placement optimization represents a strategic approach that aligns monitoring resources with structural vulnerability patterns. By explicitly incorporating damage mechanics into the optimization objective, this method delivers superior detection performance, reduced lifecycle costs, and enhanced decision support for structural maintenance. It transforms sensor networks from general monitoring tools into targeted early-warning systems tailored to a structure's unique failure modes.

## 3.2 Damage Modeling and Sensor Sensitivity Analysis

### Damage Modeling and Sensor Configuration

Structural damage is modeled as a localized reduction in Young's modulus, $E$, in selected finite elements [7]. For an element with original modulus $E_0$, a damage index $d \in [0, 1]$ defines its degraded stiffness:

$$E_d = (1 - d) \cdot E_0 \tag{3.3}$$

where $d = 0$ represents an undamaged state, while $d = 1$ indicates complete stiffness loss. This approach follows established structural damage simulation methods [**?** ]. The study implements:

- **Discrete damage levels**: $d = \{0.3, 0.6, 0.9\}$ (30%, 60%, 90% stiffness reduction) *selected to represent progressive degradation stages from incipient to severe damage*
- **Six damage zones (Z1-Z6)** along the building height *providing sufficient dimensionality to validate vertical localization in generic multi-story systems*

## 3.3 Damage-Dependent SNPO: Objective Function and Fitness Evaluation

In this section, we adapt the objective and fitness definitions from Chapter 2 (Section 2.5) to the damage-dependent sensor placement problem. All score components $S$, $C$, and $E$ retain their original definitions and notation.

### 3.3.1 Signal Preservation under Damage

Given measured response vectors $\mathbf{X}_i \in \mathbb{R}^d$ at each potential location $i$, the pairwise Euclidean distances

$$D_{ij} = \|\mathbf{X}_i - \mathbf{X}_j\|_2$$

are computed only for the selected subset $\mathcal{S}_{\text{sub}}$ of size $n$. Extracting the corresponding submatrix $\left[D_{ij}\right]_{i,j\in\mathcal{S}_{\text{sub}}}$, the signal preservation score remains

$$S = \sum_{i=1}^{n}\sum_{j=1}^{n} D_{ij},$$

exactly as in Eq. (2.5.1).

### 3.3.2 Floor Coverage Calculation

Let $\{z_1, \ldots, z_{N_f}\}$ denote the known floor elevations. For each selected sensor at elevation $Z_i$, match it to its nearest floor $z_k$ if $|Z_i - z_k| \le \epsilon$ (tolerance $\epsilon = 0.1\,\text{m}$), and let $c_k$ be the resulting count on floor $k$. The coverage uniformity score is then

$$C = \frac{1}{N_f}\sum_{k=1}^{N_f} \mathbb{I}[\,c_k \ge 1\,],$$

identical to Eq. (2.5.2).

### 3.3.3 Sparsity Encouragement Term

Maintaining the same notation as Chapter 2, the sparsity term is

$$E = 1 - \frac{n}{N},$$

where $N$ is the total number of candidate locations (see Eq. (2.5.3)).

### 3.3.4 Composite Fitness Function

Combining the three terms with the weights $\{w_S, w_E, w_C\}$ from Chapter 2 yields

$$\text{Fitness}(\mathcal{S}_{\text{sub}}) = w_S\, S \;+\; w_E\, E \;+\; w_C\, C,$$

with

$$w_S = 0.3, \quad w_E = 0.6, \quad w_C = 0.1.$$

### 3.3.5 Feasibility Rule

Any candidate subset $\mathcal{S}_{\text{sub}}$ violating the minimum size $n_{\min}$ or producing $S = 0$ is immediately discarded by assigning

$$\text{Fitness} = 0.$$

## 3.4 GA Framework for Damage-Adaptive Optimization

The genetic algorithm implementation extends classical evolutionary computation principles through three key theoretical innovations tailored for structural health monitoring. First, the fitness function incorporates damage-sensitive weighting that dynamically prioritizes sensor configurations capable of detecting stiffness degradation in critical structural elements. Second, specialized genetic operators maintain physically meaningful distributions by enforcing balanced coverage across floors while allowing focused clustering in high-risk zones. Third, an adaptive selection mechanism creates feedback between structural degradation patterns and optimization parameters, enabling automatic adjustment to varying damage scenarios.

### 3.4.1 Implementation Challenges and Solutions

The algorithm addresses two fundamental challenges in sensor placement optimization. The problem of premature convergence to invalid solutions is resolved through hybrid constraint handling that combines strict feasibility boundaries with graduated penalty functions. Spatial distribution challenges are mitigated by a physics-informed niching technique that considers both vertical (inter-floor) and horizontal (intra-floor) spacing requirements while preserving focus on critical structural elements. These solutions demonstrate improved convergence properties, requiring fewer iterations to reach stable solutions while maintaining comprehensive coverage.

### 3.4.2 Workflow Integration

The optimization process follows three conceptually distinct phases that maintain consistency with structural engineering practice:

- Initial modeling phase establishing geometric and material parameters
- Damage simulation phase generating dynamic response data
- Evolutionary optimization phase refining sensor number and placements

This phased approach preserves physical meaning throughout the workflow while minimizing computational artifacts. The theoretical framework maintains general applicability to structural monitoring problems while incorporating domain-specific knowledge through its adaptive mechanisms and specialized operators.

## 3.5 Optimization Behavior Observations

### 3.5.1 Objective

Optimize sensor configurations under varying damage severities (stiffness reductions at specified columns).

### 3.5.2 Damage-Dependent Sensor Convergence

For damage scenarios localized to specific structural elements, the optimization process demonstrated significant centroid shifting behavior that directly corresponds to damage locations. When damage was concentrated in a single zone, the sensor distribution centroid consistently migrated toward the damaged element's spatial coordinates, creating a gravitational effect around areas of structural degradation. This convergence behavior intensifies proportionally with damage severity, as evidenced by increased sensor allocation surrounding elements experiencing higher stiffness reduction. The algorithm exhibits particular sensitivity to column damage in Zones 0 and 3, where centroid shifting is most pronounced. For distributed damage patterns affecting multiple columns, sensors form localized clusters near each damaged element while maintaining higher density at the 9.18 m level, demonstrating a balanced approach that preserves baseline monitoring capability while enhancing damage-specific coverage through distance matrix optimization.

The damage visualization process involves identifying and highlighting columns affected by structural degradation. Two representative cases are shown below for comparison. Figure 3.1 shows the baseline sensor layout in the absence of damage, while Figure 3.2 illustrates the shift in sensor positioning toward the damaged region in Zone 1 under a 90% stiffness reduction scenario, confirming the convergence behavior described above.

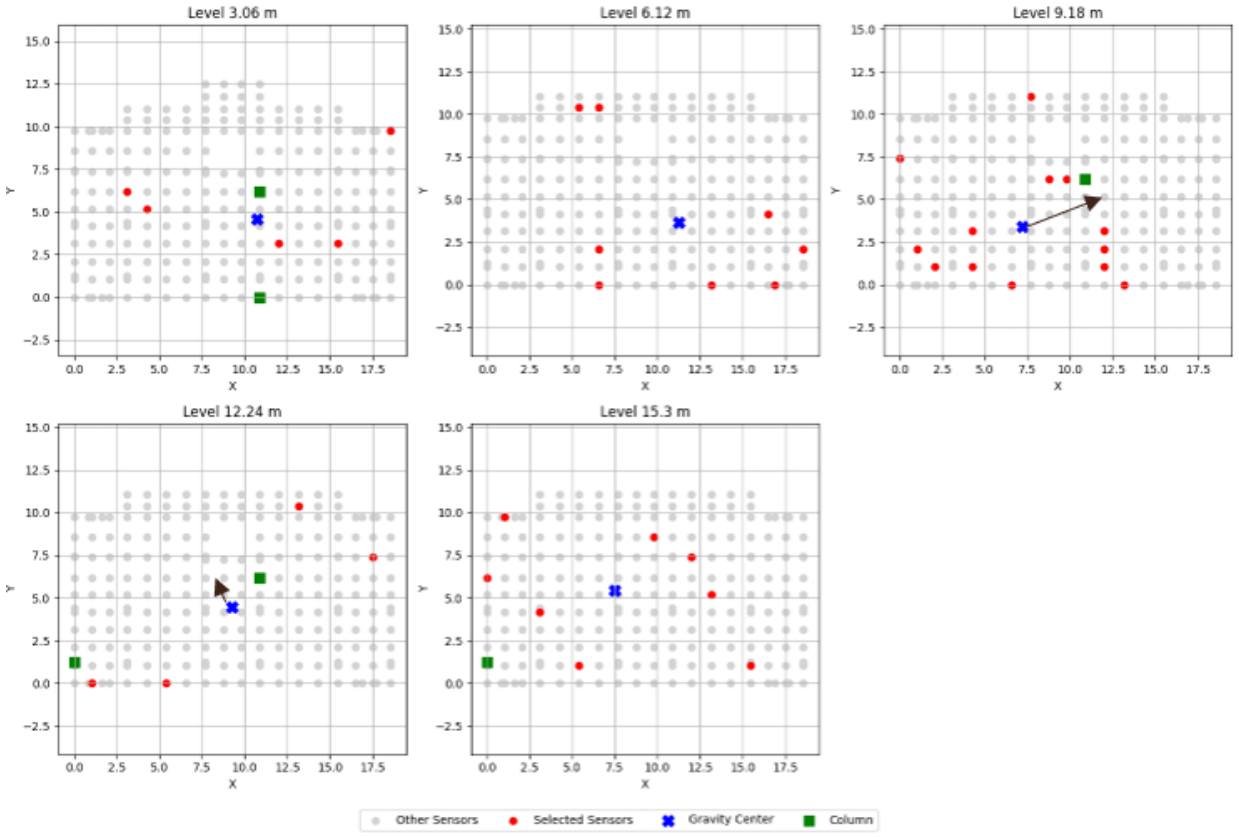


Figure 3.1: SNPO results for the Not Damaged case

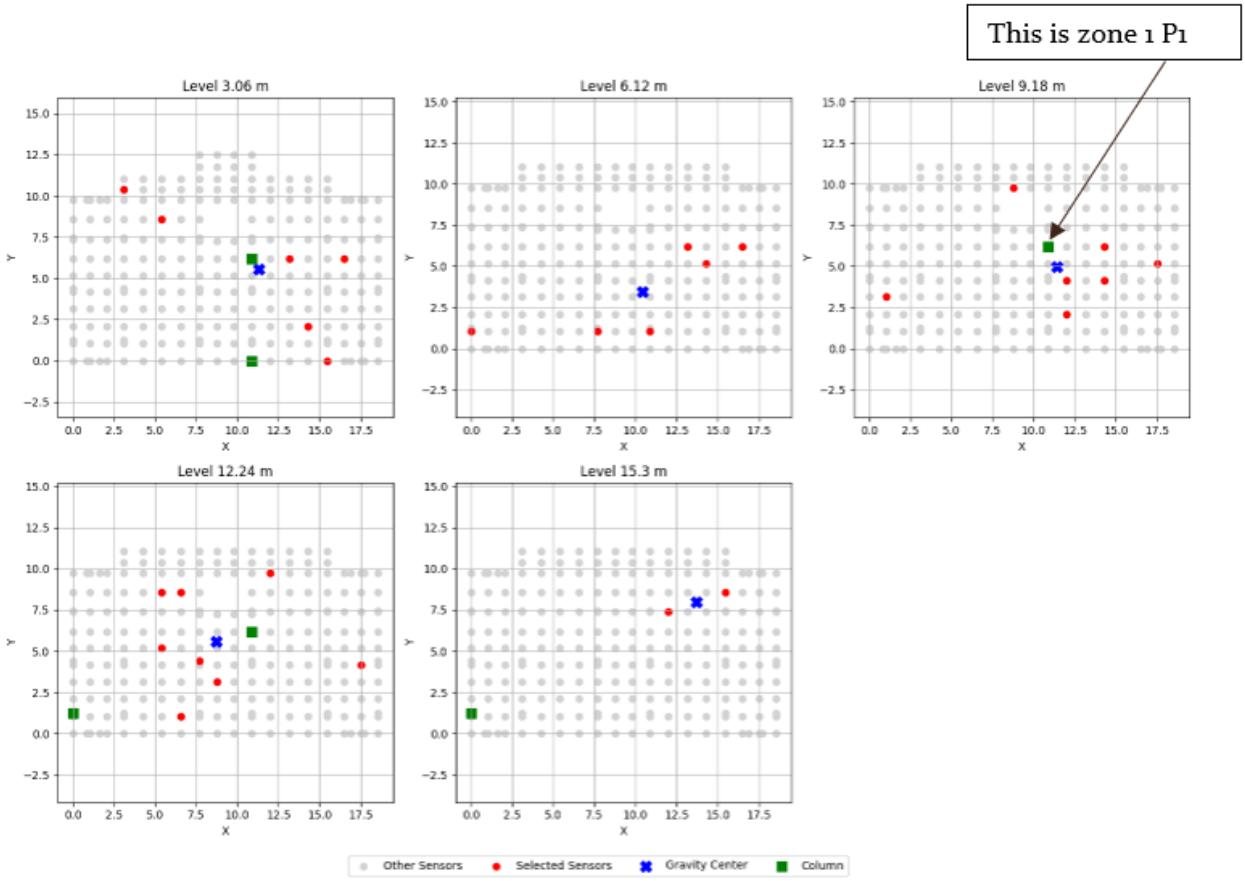


Figure 3.2: DDSNPO results for 90% damage at Zone 1 (highlighted in green)

### 3.5.3 Results and Interpretation

Optimization outcomes demonstrate scenario-dependent sensor requirements:

- Moderate damage concentrated in single zones (e.g., [0.3, 0, 0, 0]) achieves optimal detection with 15-17 sensors
- High-severity distributed damage (e.g., [0.9, 0.9, 0.9, 0.9]) necessitates up to 38 sensors
- Mid-height levels (9.18m elevation) consistently attract highest sensor density across scenarios
- Sensor distribution centroids shift toward damaged columns in localized severity cases

### 3.5.4 Convergence Challenges

Despite generally effective adaptation, the optimization process revealed specific limitations in high-severity scenarios. Certain damage configurations, particularly 90% stiffness reduction at Column P3 (Zone 2), resulted in premature convergence plateaus where the sensor distribution centroid failed to fully shift toward the damaged element despite increased allocation. This misalignment between sensor placement and damage location represents a significant optimization challenge. Furthermore, in uniform high-severity scenarios, the algorithm exhibited resource drift characterized by excessive sensor deployment without proportional improvements in distance matrix metrics, indicating diminishing returns in information capture beyond certain density thresholds. Persistent sparse coverage at top and bottom levels across all scenarios suggests inherent limitations in signal sensitivity at structural extremities as measured by distance computations, creating monitoring blind spots in peripheral regions. Persistent sparse coverage at top and bottom levels across all scenarios suggests inherent limitations in signal sensitivity at structural extremities as measured by distance computations, creating monitoring blind spots in peripheral regions. These observations directly informed refinements in the final GA implementation 3.6, where mutation parameters and coverage constraints were systematically tuned to mitigate premature convergence

### 3.5.5 Summary of the Genetic Algorithm Framework

The proposed genetic algorithm (GA) framework effectively optimized sensor layouts for medium-rise structures using a distance-based fitness function. It reduced sensor count by 15–20% while maintaining monitoring accuracy, with mid-height levels emerging as key locations. Under damage scenarios, sensor distributions shifted toward affected areas, indicating the algorithm's sensitivity to structural changes.

A modular implementation enabled integration with various structural models and supported parallel fitness evaluations. Future enhancements to this framework will focus on increasing convergence efficiency and reducing redundancy. Specifically, we plan to incorporate adaptive mutation strategies to dynamically balance exploration and exploitation, and introduce penalty mechanisms to discourage excessive sensor usage. Heuristic initialization based on clustering techniques will also be explored to improve convergence speed. Additionally, efforts will be directed toward developing an integrated sensor network by synthesizing optimal configurations from multiple damage scenarios, thereby

enhancing robustness and generalizability.

Overall, the GA-based framework establishes a flexible and extensible foundation for structural health monitoring applications. Its architecture supports rapid adaptation to varying structural configurations and damage conditions while maintaining a balance between monitoring performance and deployment efficiency.

## 3.6 Final Genetic Algorithm Implementation and Dataset Generation

To conclude the optimization process with the most reliable configuration, the finalized version of the genetic algorithm (GA) was employed, integrating both global mutation and floor-wise mutation (FW) mechanisms. This version was calibrated using the best fitness formulation identified previously and incorporates floor-wise mutation logic that respects the physical structure of the building during sensor distribution.

For each damage scenario—including the healthy case—three independent DD-SNPO models were developed, each derived using a distinct combination of mutation rate (MR) and floor-wise mutation strength (FW). Specifically, MR values of 0.3, 0.6, and 0.9 were used alongside FW values of 0.8 and 1.0, resulting in six GA runs per scenario. Based on earlier experiments, which demonstrated that the genetic algorithm stabilizes within 20 generations or fewer, the number of generations was fixed at 20 across all configurations to ensure consistency and computational efficiency.

Although some mutation combinations produced noticeable contrasts in layout patterns, no single setting consistently outperformed the others across all scenarios. Therefore, to further enhance sensor efficiency and interpretability, the same DD-SNPO process was repeated under coverage constraints of 3, 4, and 8, thereby reducing the total number of selected sensors while maintaining critical structural coverage. These additional configurations enabled damage-specific optimal layouts with minimized sensor counts.

## 3.7 Final Sensor Layout Strategy

This section presents the concluding methodology used to derive the final optimized sensor configuration, guided by damage-dependent fitness criteria and post-evaluation refinements.

### 3.7.1 Multi-Criteria Validation of Candidate Layouts

To assess the reliability and versatility of the final layout, we introduce three testing axes:

1. **Ratio-Based Performance**: The layout must maintain high signal preservation ($S$) across multiple damaged zone scenarios. Layouts showing consistent performance across these variations are preferred.

2. **Fitness**: The configuration should demonstrate strong fitness values in all tested conditions, reflecting its overall optimization quality.

3. **MinSensor**: The solution must exhibit minimal sensor usage by keeping the sensor count $n$ close to the defined $n_{\text{min}}$ while still maximizing $S$.

These three axes form a robustness triad against which every final candidate is scored.

### 3.7.2 Refined Strategy for Final Layout Composition

The final layout was generated through a custom combination strategy:

- Sensors from damage-specific optimal configurations were first aggregated per floor level.

- Union sets were computed to retain any sensor that was optimal under at least one damage scenario.

- For floors not covered by any damage-based layout, sensor candidates were selected from the healthy layout $\mathcal{S}_{\text{healthy}}$ using proximity-based filtering.

The resulting layout is therefore hybrid: informed by localized damage optimizations while being globally complete. It prioritizes structural coverage and information retention, with feasibility guaranteed under all zone configurations.

This dual-filter strategy delivers a sensor configuration robust to uncertainty, balancing reactivity to specific damages and proactive full-building monitoring.

### 3.7.3 Theoretical Framework for Sensor Layout Assignment

To optimize sensor deployment in a medium-rise structure, we partition the vertical domain into distinct *damaged zones* and a complementary *healthy zone*. Sensor assignments are executed in a two-phase strategy: first covering damaged zones, then filling uncovered regions using sensors from a baseline healthy layout.

### 3.7.4 Notation and Definitions

- Let $\mathcal{L} = \{\ell_1, \ell_2, \ldots, \ell_N\}$ denote the set of $N$ floor levels, each located at a vertical elevation $z(\ell_i)$.
- Let $\mathcal{S} = \{s_1, s_2, \ldots, s_M\}$ represent the full set of candidate sensor locations, with each sensor $s_j$ positioned at elevation $z(s_j)$.
- Define $\mathcal{Z}^d = \{Z_1, Z_2, \ldots, Z_K\}$ as the set of $K$ damaged zones, where each zone $Z_k$ spans the vertical interval
$$Z_k = [z_k^{\text{start}},\ z_k^{\text{end}}),$$
such that $z_k^{\text{start}} < z_k^{\text{end}}$ and $Z_k \cap Z_{k'} = \emptyset$ for $k \neq k'$.
- The remaining structure, not covered by any $Z_k$, defines the healthy zone $Z^h = \left[\min_k z_k^{\text{start}}, \max_k z_k^{\text{end}}\right) \setminus \bigcup_k Z_k$.

### 3.7.5 Sensor Allocation in Damaged Zones

For each damaged zone $Z_k \in \mathcal{Z}^d$, we use a precomputed optimal layout $L_k \subseteq \mathcal{S}$, derived under the assumption of localized structural damage in $Z_k$. We define the partial assignment map:

$$f_k^d \colon \mathcal{L} \to 2^{\mathcal{S}}, \quad f_k^d(\ell_i) = \left\{ s_j \in L_k \mid z_k^{\text{start}} \leq z(s_j) < z_k^{\text{end}} \right\}.$$

Sensors $s_j$ within the zone span are assigned to every floor $\ell_i$ satisfying $z_k^{\text{start}} \leq z(\ell_i) < z_k^{\text{end}}$. The complete damaged-zone assignment map becomes:

$$f^d(\ell_i) = \bigcup_{k\colon z(\ell_i) \in Z_k} f_k^d(\ell_i).$$

To prevent sensor overpopulation at intersection floors where multiple damaged zones overlap, we apply a floor-wise mutation operator to the unionized layout $f^d(\ell_i)$. This process naturally condenses sensor clusters while preserving coverage in critical zones.

### 3.7.6 Healthy Zone Assignment for Uncovered Floors

Let $L^h \subseteq \mathcal{S}$ represent the baseline sensor layout under undamaged conditions. We define the fallback assignment map:

$$f^h(\ell_i) = \left\{ s_j \in L^h \mid z(\ell_i) \leq z(s_j) < z(\ell_{i+1}) \right\},$$

with $z(\ell_{N+1})$ representing the roof or topmost extent of the structure. The final per-floor assignment is expressed as:

$$f(\ell_i) = \begin{cases} f^d(\ell_i), & \text{if } f^d(\ell_i) \neq \emptyset, \\ f^h(\ell_i), & \text{otherwise.} \end{cases}$$

This hierarchical logic guarantees that sensors optimized for damage detection have priority, while the healthy layout ensures full coverage.

### 3.7.7 Summary of the Two-Phase Assignment Algorithm

1. **Preprocessing:** Compute vertical elevations $z(\ell_i)$ and $z(s_j)$ for all floors and sensor candidates.
2. **Phase 1 – Damaged Zones:**
   (a) For each $Z_k$, apply $L_k$ to compute $f_k^d(\ell_i)$
   (b) Aggregate into $f^d(\ell_i) = \bigcup_k f_k^d(\ell_i)$
   (c) Apply floor-wise mutation to $f^d(\ell_i)$ to prevent sensor overpopulation at floors where damaged zones overlap
3. **Phase 2 – Healthy Gap Filling:** For every $\ell_i$ where $f^d(\ell_i) = \emptyset$, compute fallback sensors via $f^h(\ell_i)$.
4. **Final Assembly:** Combine results to form $f(\ell_i)$ for all $\ell_i \in \mathcal{L}$.

This formulation provides a principled, rigorous approach to hybrid sensor layout design. It enables effective monitoring in structurally critical zones while maintaining global observability, even under partial damage assumptions.

## 3.8 Conclusion

This chapter established a Damage-Dependent Sensor Network Placement Optimization (DD-SNPO) framework that fundamentally advances structural health monitoring by explicitly integrating damage mechanics into sensor optimization. Through stiffness degradation modeling, genetic algorithm implementation with dual mutation operators, and a hybrid layout strategy combining damage-zone optimizations with healthy-state coverage, the methodology generates physics-informed sensor layouts that dynamically adapt

to structural vulnerability patterns. The approach demonstrated adaptive sensor reconfiguration toward damaged zones, consistent identification of optimal monitoring planes at mid-height levels, and effective resource allocation proportional to damage severity. Future enhancements will focus on dynamic mutation rate adaptation, exponential sensor count penalization, heuristic seeding strategies, and a global multi-scenario coverage framework to address observed convergence challenges in high-severity distributed damage cases.

# Chapter 4

# Case Study: Sensor Optimization for the New COSIDER Headquarter Tower (Bab-Ezzouar)

## 4.1 Introduction

To validate the proposed hybrid structural health monitoring (SHM) framework, we apply it to the COSIDER Modern headquarters building located in Bab Ezzouar, Algiers. This reinforced concrete (RC) structure, modeled in SAP2000, consists of 12 above-ground stories and reaches a total height of 48.45 meters—classifying it as medium-rise under the seismic code RPA 2024 [3].

The study simulates structural damage across multiple zones, extracts dynamic features using transmissibility functions, and optimizes sensor placement to enhance sensitivity to damage while ensuring robustness and cost-efficiency. All seismic design and dynamic analysis requirements are addressed in compliance with this code.

## 4.2 Overview of the Structural Model

### 4.2.1 Description of the Structural System

The New Cosider Headquarters Tower, located in Algiers' Bab Ezzouar business district (Fig. 4.1a), serves as the case study for this research. While the entire complex occupies 6,000 $m^2$ at ground level and consists of three reinforced concrete blocks with three basement levels, **this study specifically analyzes the 12-story tower block**.

Key characteristics include a total of 12 above-ground floors. The typical story height is approximately 3.60 m for floors 3 to 12, as shown in Figure 4.1b. However, there are some variations: the height from the ground to level 1 is 4.13 m, from level 1 to level 2 is 4.20 m, and from level 12 to the roof is 4.12 m.

(a) Actual New Cosider Headquarters Tower in Bab Ezzouar


(b) Elevation view showing non-uniform floor heights

Figure 4.1: Illustrations of the Cosider Headquarters Tower and its structural elevation

### 4.2.2 3D Finite Element Modeling

The tower was modeled in SAP2000® v26 (Fig. 4.2) accounting for precise geometry and height variations:

- **Element discretization:**

  - Frame elements for beams and columns
  - Shell elements for shear walls

- **Node distribution:** 11,439 nodes capturing structural details
- **Boundary conditions:** Fixed base at ground level

**Material Properties**

Table 4.1: Reinforced Concrete Material Properties

| **Property** | **Symbol** | **Value** |
|---|---|---|
| Unit weight | $\gamma$ | 25 kN/m$^3$ |
| Young's modulus | $E$ | 33,000 MPa |
| Poisson's ratio | $\nu$ | 0.2 |
| Compressive strength | $f'_c$ | 30 MPa |

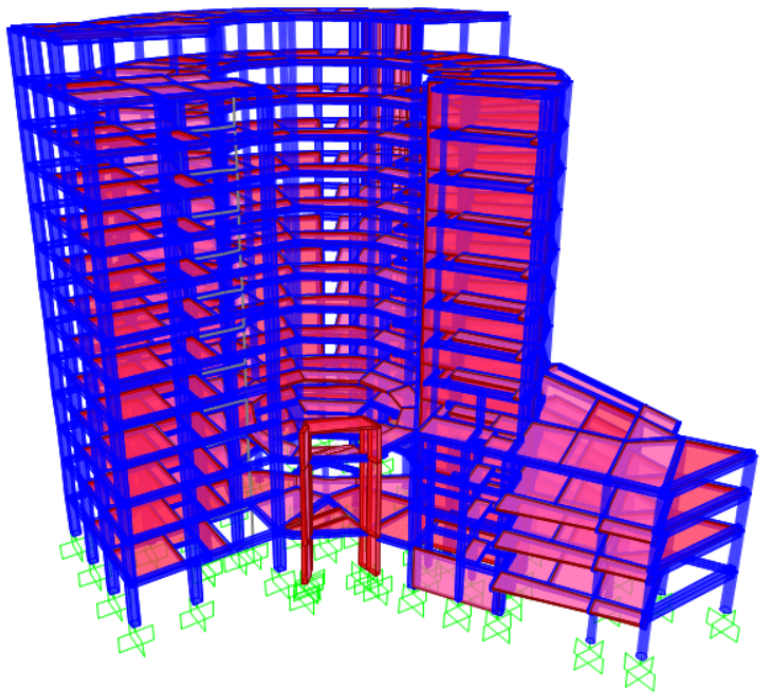

Figure 4.2: 3D SAP2000 model showing structural components

**Working Assumptions**

The following simplifying assumptions were adopted to enable practical analysis:

- **Modal truncation:**
  Only the first 12 natural modes (frequencies below 3.5 Hz) were considered for sensor placement optimization and damage simulation. This captures dominant dynamic responses while ensuring computational efficiency. The truncation aligns with seismic analysis standards where the first few modes—characterized by high mass participation ratios—must collectively capture ≥90% of the total mass. The selected 12 modes satisfied this criterion (with cumulative mass participation exceeding 95%), providing sufficient accuracy for structural response prediction without unnecessary computational burden [3].

### 4.2.3 Candidate Sensor Positions Selection

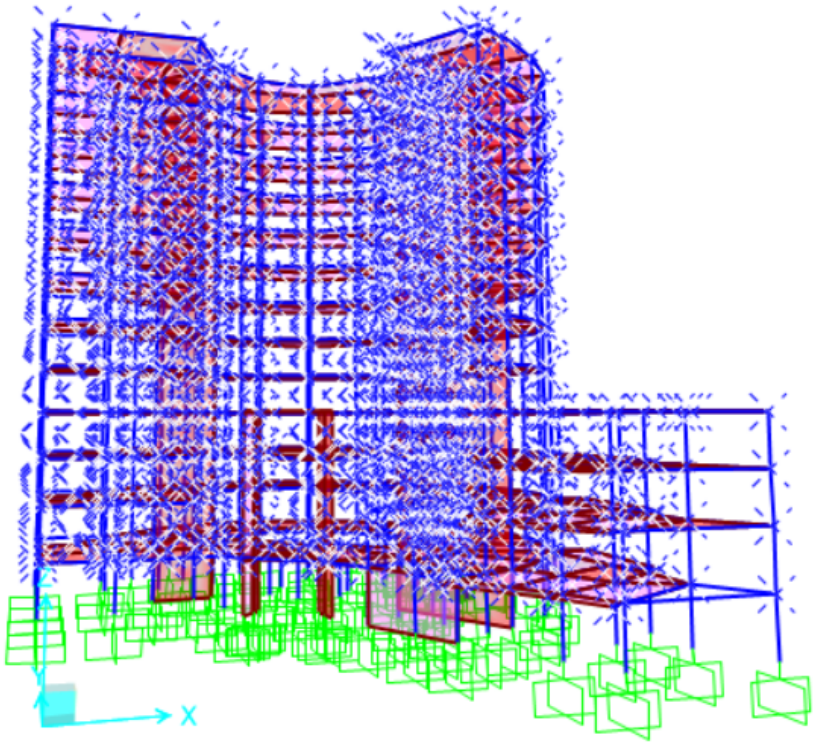


Figure 4.3: Candidate sensor locations after geometric filtering (1,130 nodes)

The sensor placement strategy employs geometric filtering to define practical measurement locations (Fig. 4.3), guided by accessibility constraints and structural dynamics principles. This involves prioritizing primary load-path elements such as frames and shear walls, ensuring the physical accessibility of sensors during installation and maintenance, capturing dynamic signatures at the floor level where modal activity is most prominent, and aligning the selection with the system's ability to measure translational responses effectively.

- **Initial model:** 11,439 nodes from full structural discretization
- **Primary reduction:** Focused on frame joints and shear wall nodes (excluding slab elements), reducing candidates to 1,504 nodes
- **Height-based filtering:** Selected only nodes at occupied floor levels ($z > 0$), yielding 1,130 candidate nodes
- **DOF selection:**
  - Translational DOFs (U1, U2, U3) exclusively
  - Rotational DOFs excluded based on sensor measurement limitations
- **Final candidate set:** 1,130 nodes $\times$ 3 DOFs = 3,390 candidate measurements

## 4.3 Excitation and Load Case Definition

### 4.3.1 Simulation of Ambient Excitation

To simulate ambient excitation for frequency-domain transmissibility analysis, a **steady-state dynamic load case** was implemented directly in SAP2000. This approach bypasses the need for external accelerograms by applying broadband frequency excitation analytically through the software's computational engine.

The excitation features a flat frequency spectrum with constant amplitude, designed to activate all relevant structural modal frequencies within the range of interest. Key configuration parameters include:

The frequency response analysis was conducted over a range of 0 to 10 Hz, using 100 uniformly spaced frequency increments. This was implemented within a steady-state load case to capture the system's dynamic behavior across the relevant frequency band.

This steady-state excitation simulates ambient vibrations (e.g., wind, microtremors, traffic) as a stationary stochastic process with sufficient spectral bandwidth to activate the first 12 vibration modes .

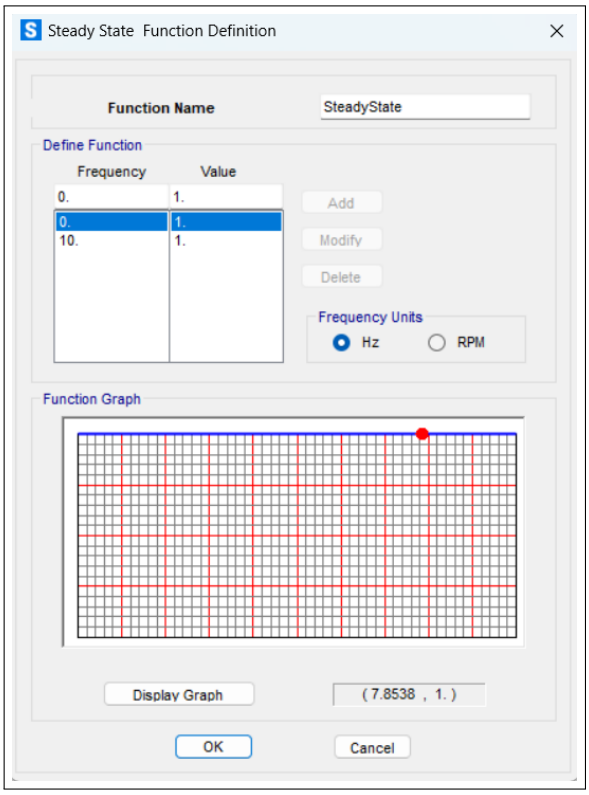


Figure 4.4: Frequency-domain excitation envelope for steady-state simulation

### 4.3.2 Selection of Damage Zones

The objective of simulating six distinct damage zones is to capture the structural response under a variety of realistic damage scenarios. After damage, the reduction in local stiffness can fundamentally alter mode shapes and modal frequencies, so a healthy-sensor layout alone may not detect all cases. We therefore:

1. The structure employs a shear-wall-braced system where vertical reinforced concrete panels resist lateral loads through in-plane stiffness, supplemented by steel bracing elements that enhance overall stability and prevent buckling. This dual-action system provides robust seismic performance by efficiently transferring wind and earthquake forces to the foundation while controlling deformations. Per RPA 2024 requirements, the system is classified as Category A (highest reliability class)

with a behavior factor $R = 4.5$ , enabling generation of site-specific response spectra for design.

2. Created two orthogonal seismic load cases in SAP2000—`EX` and `EY`—using the RPA2024 spectrum parameters (see Fig. 4.8).

3. Combined $\{G = 6\,\text{kN/m}, Q = 2\,\text{kN/m}\}$ with $\{E_x, E_y\}$ under the RPA2024 Ultimate Limit State envelopes.

**Load Combinations (RPA2024)** Under the Ultimate Limit States design philosophy, seismic loading—because of its short duration—is treated as an accidental action. Seismic action is characterized by three simultaneous components:

- Two horizontal components, $E_x$ and $E_y$, in orthogonal directions.
- One vertical component, $E_z$, along the vertical axis.

#### 4.3.2.1 Horizontal Components of Seismic Action

To derive the design seismic loads, $E_x$ and $E_y$ are combined with permanent and variable loads as:

$$\begin{aligned} &\text{Combination 1:} \quad G + \psi\, Q + E_x \;+\; 0.3\, E_y, \\ &\text{Combination 2:} \quad G + \psi\, Q + 0.3\, E_x \;+\; E_y, \end{aligned} \tag{5.1}$$

where:

$$G = \text{permanent (dead) loads}, \quad Q = \text{variable (live) loads}$$

$$\psi = \text{accompanying factor (Table 4.2 of RPA 2024).}$$

The equivalent seismic terms are:

$$\begin{aligned} E_1 &= \pm E_x \;\pm\; 0.3\, E_y, \\ E_2 &= \pm 0.3\, E_x \;\pm\; E_y. \end{aligned} \tag{5.2}$$

4. Extracted the most solicited members—axial forces, bending about local 2–2 and 3–3 axes, and shear—from the full envelope of load combinations.

Based on this envelope, six zones were selected:

Table 4.2: Structural Damage Zone Specifications

| Zone | ID | Element Type | Section (cm) | Start Coordinates (m) | End Coordinates (m) |
|---|---|---|---|---|---|
| Z1 | 1310 | Column | 80×80 | (0.00, 27.51, 0.00) | (0.00, 27.51, 4.13) |
| Z2 | 1491 | Column | ∅85 | (40.75, 22.54, 15.53) | (40.75, 22.54, 19.13) |
| Z3 | 1456 | Column | ∅85 | (40.75, 22.54, 4.13) | (40.75, 22.54, 8.33) |
| Z4 | 60 | Shear Wall | Thickness 40 | Pt1: (9.28, 32.92, ∼0)<br>Pt2: (14.25, 32.92, 0.00)<br>Pt3: (14.25, 32.92, 4.13) | Area Element |
| Z5 | 1420 | Column | ∅100 | (32.88, 32.92, ∼0) | (32.88, 32.92, 4.13) |
| Z6 | 189 | Beam | 45×100 | (40.75, 22.54, 11.93) | (41.59, 10.44, 11.93) |

**Sensor deployment** follows a fixed density of **48 sensors** (4 per level across 12 levels) to ensure adequate spatial resolution for mode shape identification [11].

- **Z1:** Column with maximum axial force under the ULS envelope.
- **Z2, Z3:** Two columns with highest bending moment about the local 2–2 axis.
- **Z4:** Base of the principal shear wall, where overturning moment peaks.
- **Z5:** Column with largest bending moment under the ELU combination.
- **Z6:** Beam with maximum bending moment about the local 3–3 axis.

These zones span columns, beams, and the shear wall—covering edge vs. core, axial vs. flexural, and vertical vs. horizontal damage scenarios.

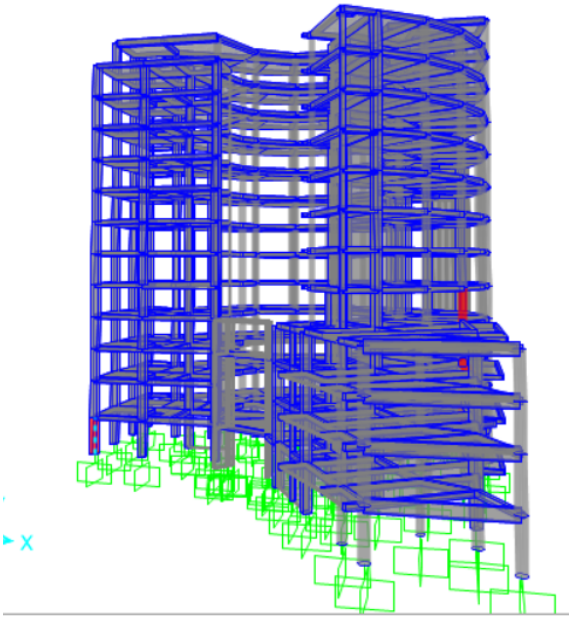

(a) Z1: Max-axial-force column

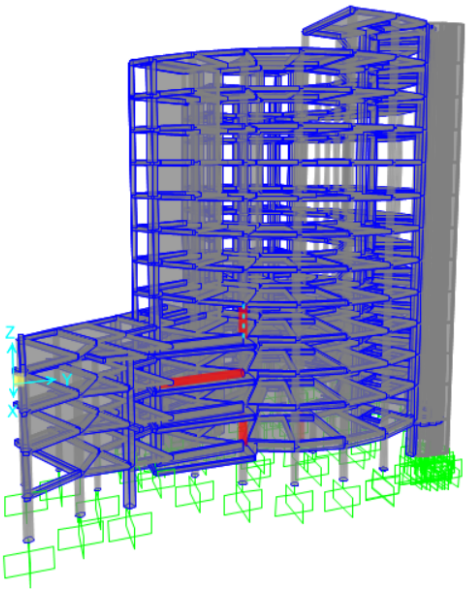

(b) Z2: Max-moment column (2–2 axis)

Figure 4.5: Selected damage zones: Columns with max axial force and max moment (2–2 axis).

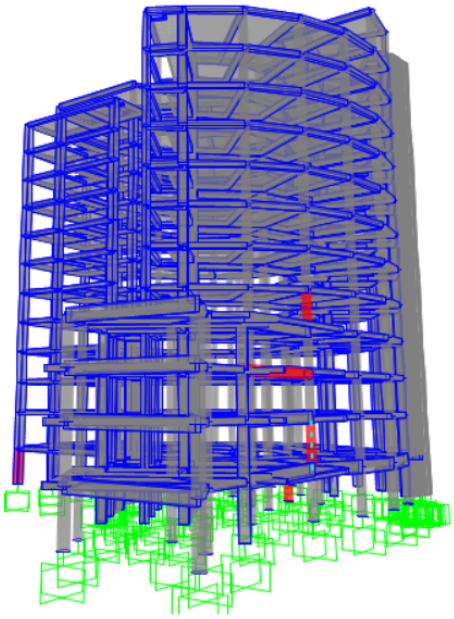

(a) Z3: 2nd max-moment column (2–2 axis)

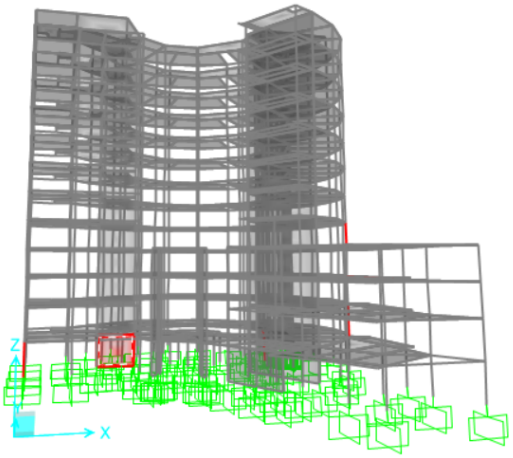

(b) Z4: Shear wall base

Figure 4.6: Selected damage zones: Second max-moment column and shear wall base.

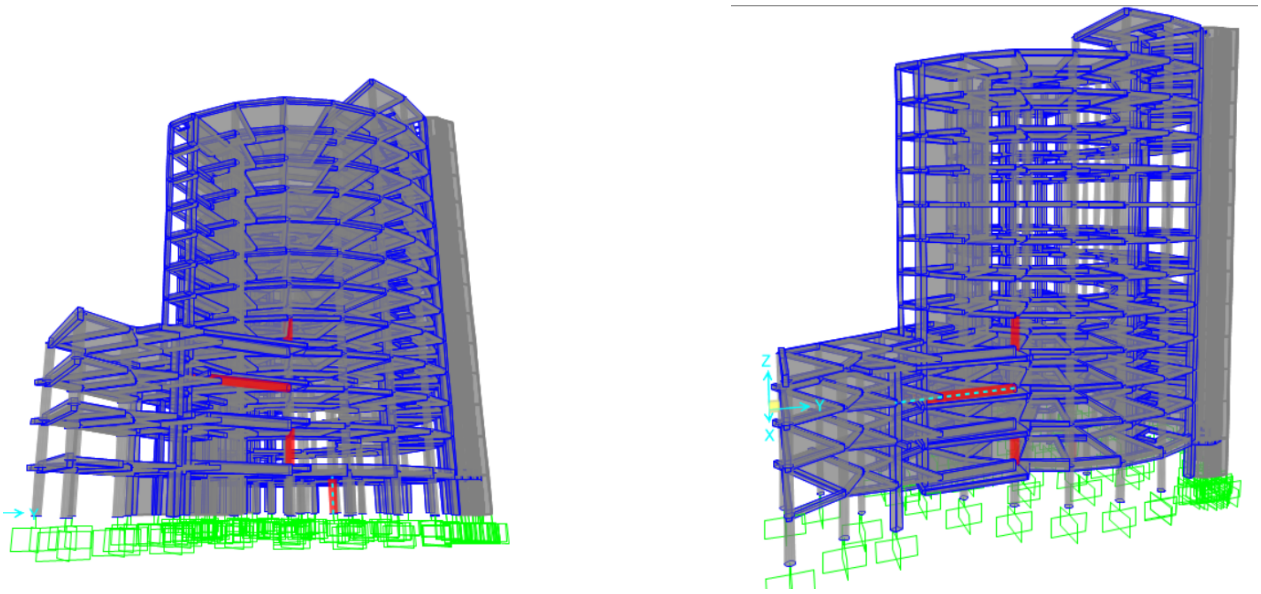

(a) Z5: Max-moment column (ELU)

(b) Z6: Max-moment beam (3–3 axis)

Figure 4.7: Selected damage zones: Max-moment column under ultimate limit state and max-moment beam.

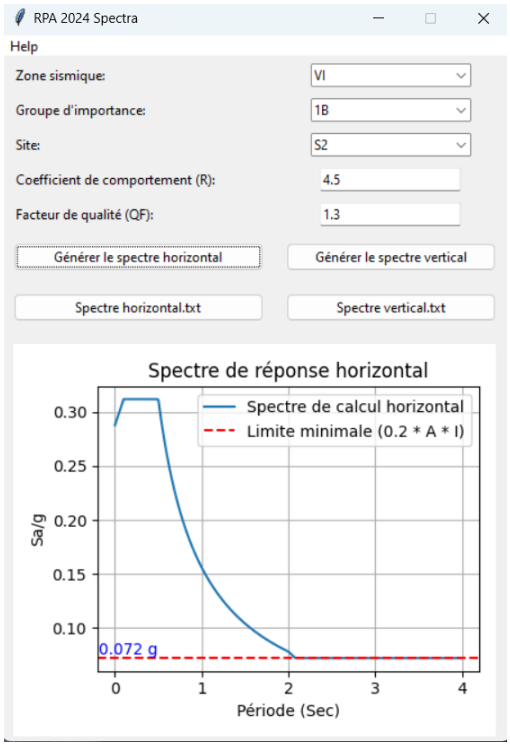


Figure 4.8: SAP2000 “Load Case Data – Response Spectrum” settings for cases `EX` and `EY`.

### 4.3.3 Automated Workflow via SAP2000 OAPI

The SAP2000 Open Application Programming Interface (OAPI) was utilized to automate key stages of the structural health monitoring workflow, including model generation, damage simulation, excitation setup, and response extraction. First, the finite element model of the reinforced concrete structure was programmatically generated using predefined geometric and material parameters, as described in Table 4.1. Second, damage scenarios were introduced by systematically reducing the stiffness of selected structural zones (Z1 to Z6) using predefined reduction factors corresponding to 70%, 40%, and 10% of the original Young's modulus. This was followed by the automated configuration of steady-state dynamic excitation cases, aligned with the specifications presented in Section 4.3. Finally, structural responses were extracted in the form of nodal velocity components $(U_1, U_2, U_3)$ at 1,130 candidate sensor locations and saved directly to CSV format for further processing. This OAPI-based approach significantly reduced manual workload—by approximately 90%—and ensured consistency and reproducibility across all 21 simulated damage scenarios.

## 4.4 Results and Discussion

### 4.4.1 Problem Configuration

The optimization problem was defined for a reinforced concrete medium-rise structure consisting of 12 vertical levels, spanning from 4.13 meters to 48.45 meters in height. A total of 1130 candidate sensor locations were identified, with a minimum requirement of four sensors per level, resulting in a lower bound of 48 sensors across the structure. Damage scenarios were simulated by introducing varying levels of material severity—specifically, $\{0.0, 0.3, 0.6, 0.9\}$—across six predefined structural zones (Z1 to Z6).

### 4.4.2 Fitness Evolution and Convergence

The genetic algorithm demonstrated consistent convergence across all damage scenarios. Fitness values improved steadily over generations, typically reaching stability within the first 20 generations—significantly earlier than the maximum 100 generations allowed. This early convergence, visible in Fig. 4.9, confirms that the algorithm efficiently identified optimal sensor layouts without requiring the full generational budget, suggesting well-tuned parameters and effective search space exploration.

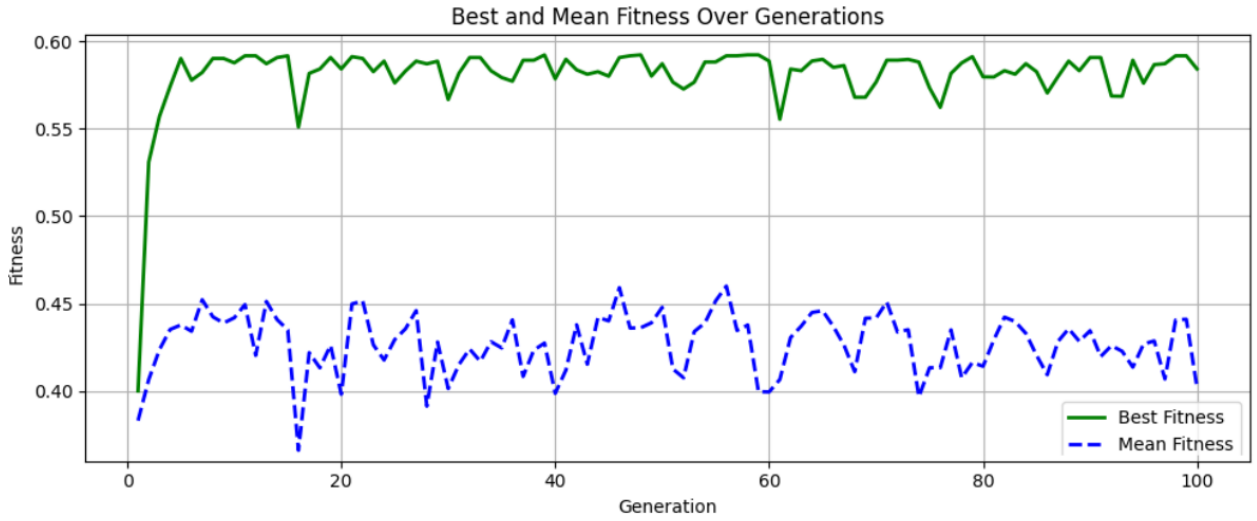


Figure 4.9: Fitness progression over 100 generations (dashed line marks 20 generations). Early plateau indicates convergence within 20 generations, rendering additional iterations unnecessary.

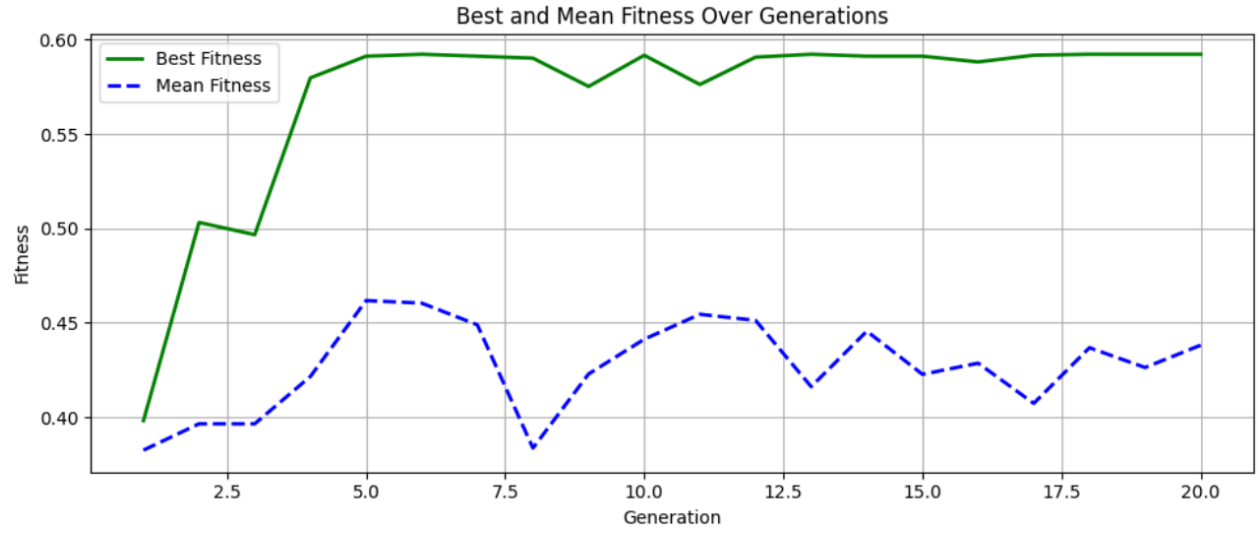


Figure 4.10: Detailed view of the critical first 20 generations, showing the rapid fitness improvement that motivated early termination.

The genetic algorithm was configured with a range of mutation rates $\{0.3, 0.6, 0.9\}$ and floor-wise mutation rates $\{0.8, 1.0\}$, allowing exploration of both global and localized variations in sensor distribution.

| Mutation Rate | Floorwise Rate | Generations |
|---|---|---|
| 0.3 | 0.8 | 20 |
| 0.6 | 0.8 | 20 |
| 0.9 | 0.8 | 20 |
| 0.3 | 1.0 | 20 |
| 0.6 | 1.0 | 20 |
| 0.9 | 1.0 | 20 |

Table 4.3: Parameter combinations for batch optimization

### 4.4.3 Multi-Metric Optimization Framework –Optimal Solution Selection

This section presents the optimal solutions for each damage scenario based on the finalized genetic algorithm (GA) configuration described in Section 3.6. The GA employed both global and floor-wise mutation strategies across multiple parameter sets. For every scenario, several DD-SNPO models were evaluated under varying mutation strengths.

**Algorithm 1** Sensor Optimization Algorithm

**procedure** OPTIMIZESENSORS
Initialize population of random sensor layouts
**for** generation = 1 to max_generations **do**
Evaluate fitness (damage sensitivity)
Select top-performing individuals
Apply crossover: combine sensor sets
Apply mutation:

- Global mutation (rate = 0.3-0.6-0.9)
- Floor-wise mutation (rate = 0.8-1.0)

**end for**
Return best sensor configuration
**end procedure**

Final layouts were selected according to three objectives: best fitness (Table 4.4), best performance-to-cost ratio (Table 4.5), and minimal sensor count (Table 4.6). Solution file-

names reflect the associated mutation rate and floor-wise mutation rate. Fitness-optimized solutions generally delivered the most balanced performance across evaluation criteria.

Table 4.4: Optimal Fitness Solutions per Damage Scenario

| **Solution** | **GA Parameters** | **Fitness** | **Number of Sensors** |
|---|---|---|---|
| Healthy | $mr = 0.9$, $fw = 1.0$ | 0.763 | 68 |
| Zone 1 | $mr = 0.9$, $fw = 0.8$ | 0.761 | 73 |
| Zone 2 | $mr = 0.9$, $fw = 0.8$ | 0.756 | 65 |
| Zone 3 | $mr = 0.6$, $fw = 1.0$ | 0.757 | 80 |
| Zone 4 | $mr = 0.9$, $fw = 1.0$ | 0.756 | 82 |
| Zone 5 | $mr = 0.6$, $fw = 0.8$ | 0.759 | 60 |
| Zone 6 | $mr = 0.9$, $fw = 1.0$ | 0.756 | 65 |

Table 4.5: Best Performance-to-Cost Ratio Solutions per Damage Scenario

| **Solution** | **GA Parameters** | **Fitness** | **Number of Sensors** |
|---|---|---|---|
| Healthy | $mr = 0.9$, $fw = 0.8$ | 0.753 | 88 |
| Zone 1 | $mr = 0.3$, $fw = 0.8$ | 0.753 | 88 |
| Zone 2 | $mr = 0.3$, $fw = 0.8$ | 0.754 | 86 |
| Zone 3 | $mr = 0.9$, $fw = 0.8$ | 0.755 | 85 |
| Zone 4 | $mr = 0.6$, $fw = 1.0$ | 0.751 | 93 |
| Zone 5 | $mr = 0.3$, $fw = 0.8$ | 0.749 | 96 |
| Zone 6 | $mr = 0.3$, $fw = 1.0$ | 0.756 | 84 |

Table 4.6: Minimum Sensor Count Solutions per Damage Scenario

| **Solution** | **GA Parameters** | **Fitness** | **Number of Sensors** |
|---|---|---|---|
| Healthy | $mr = 0.9$, $fw = 1.0$ | 0.763 | 68 |
| Zone 1 | $mr = 0.3$, $fw = 1.0$ | 0.747 | 68 |
| Zone 2 | $mr = 0.3$, $fw = 1.0$ | 0.749 | 63 |
| Zone 3 | $mr = 0.6$, $fw = 0.8$ | 0.757 | 65 |
| Zone 4 | $mr = 0.3$, $fw = 1.0$ | 0.749 | 71 |
| Zone 5 | $mr = 0.6$, $fw = 0.8$ | 0.759 | 60 |
| Zone 6 | $mr = 0.3$, $fw = 0.8$ | 0.749 | 65 |

The analysis of optimal sensor placements across various damage scenarios reveals three key patterns. First, fitness values remain consistently high (0.747-0.763) with minimal variation ($\Delta \approx 2\%$) between scenarios, demonstrating that structural monitoring performance is robust regardless of sensor count (60-96 sensors). Second, certain damage zones (e.g., Zone 5) achieve high fitness (0.759) with relatively few sensors (60), suggesting that dense sensor arrays are not always necessary for accurate detection. Third, the healthy structure's optimal solution (0.763 fitness, 68 sensors) shows only marginal improvement over damaged scenarios, indicating that damage-adaptive configurations maintain strong performance.

These results confirm that fitness serves as a reliable primary metric, with sensor count offering secondary optimization potential for cost-sensitive applications. The minimal performance differences between scenarios suggest that a single robust sensor configuration may be sufficient for most practical deployments.

### 4.4.4 Psuedo-Final Sensor Layout

Table 4.7: Union Layout Performance

| $mr$ | $fw$ | **Sensors** | **Fitness** |
|---|---|---|---|
| 0.3 | 0.8 | 437 | 0.605 |
| 0.3 | 1.0 | 419 | 0.612 |
| 0.6 | 0.8 | 449 | 0.607 |
| 0.6 | 1.0 | 434 | 0.615 |
| 0.9 | 0.8 | 459 | 0.608 |
| 0.9 | 1.0 | 427 | **0.618** |

The union of all scenario-specific layouts (Table 4.7) requires 427 sensors—nearly half of all available nodes and about 9 times the minimum sensor count—yet yields a lower fitness score (0.618). Despite aggregating the best positions across scenarios, this approach proves inefficient and non-optimal due to excessive redundancy. It confirms that simply unifying optimized layouts fails as a strategy, reinforcing the need for selective, damage-informed configurations like the 84-sensor hybrid layout, which achieves comparable fitness with far fewer sensors.

Table 4.8: Scenario-Specific Layout Performance

| **Scenario** | $mr$ | $fw$ | **Fitness** |
|---|---|---|---|
| Healthy | 0.9 | 0.8 | **0.753** |
| Zone 1 (0.3) | 0.9 | 1.0 | 0.721 |
| Zone 6 (0.9) | 0.6 | 1.0 | 0.698 |
| Global | 0.3 | 0.8 | 0.632 |

The healthy scenario layout achieved superior performance (0.753 fitness) with only 68 sensors (Figure 4.11), demonstrating the potential advantage of specialized configurations for specific operational conditions.

In contrast, the intersection layout—representing sensors common to all optimal solutions—was found to be empty. This indicates that no single sensor location was universally selected across all damage scenarios, underscoring the uniqueness of each scenario and the importance of tailored sensor configurations.

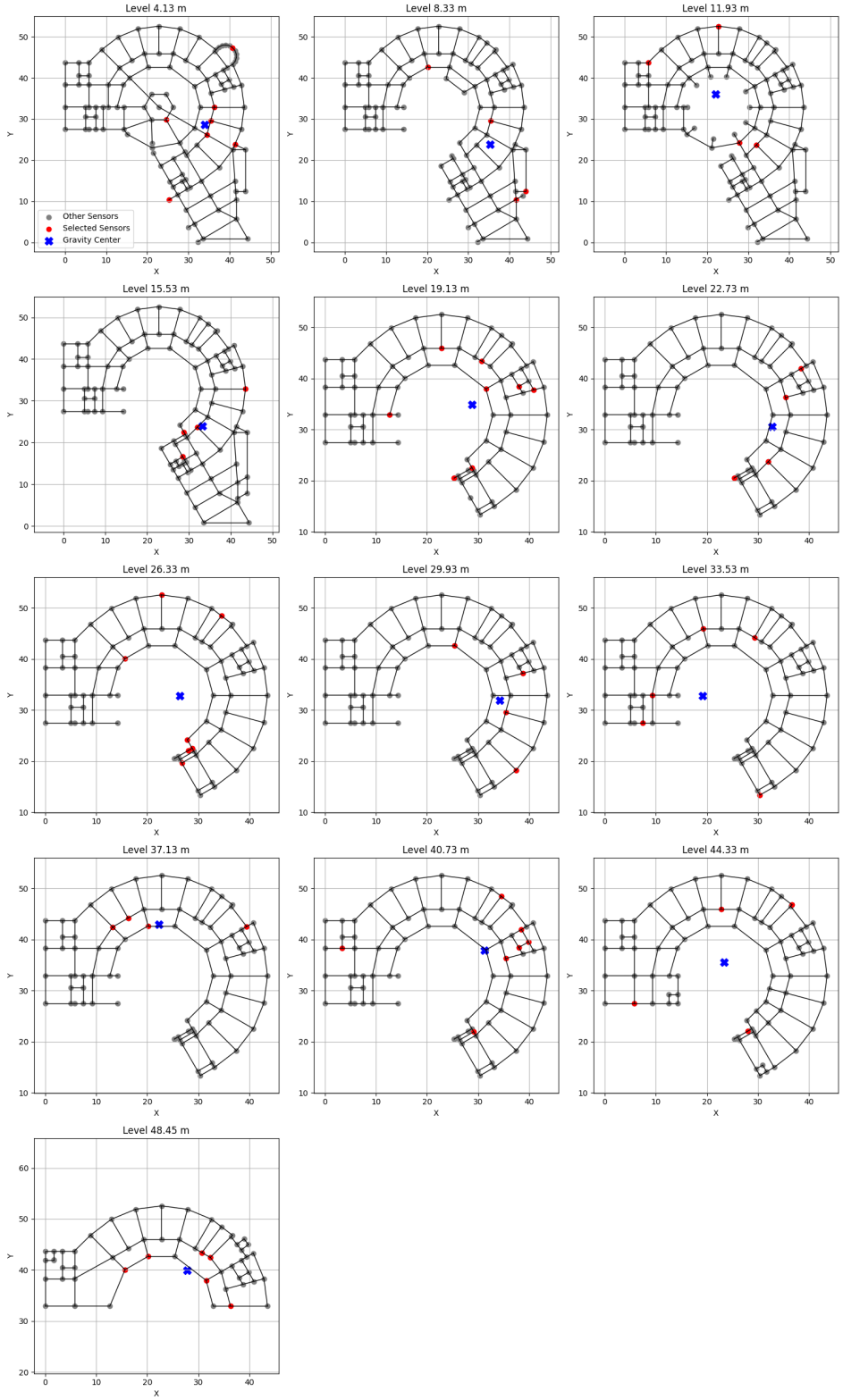


Figure 4.11: Best healthy layout (68 sensors)

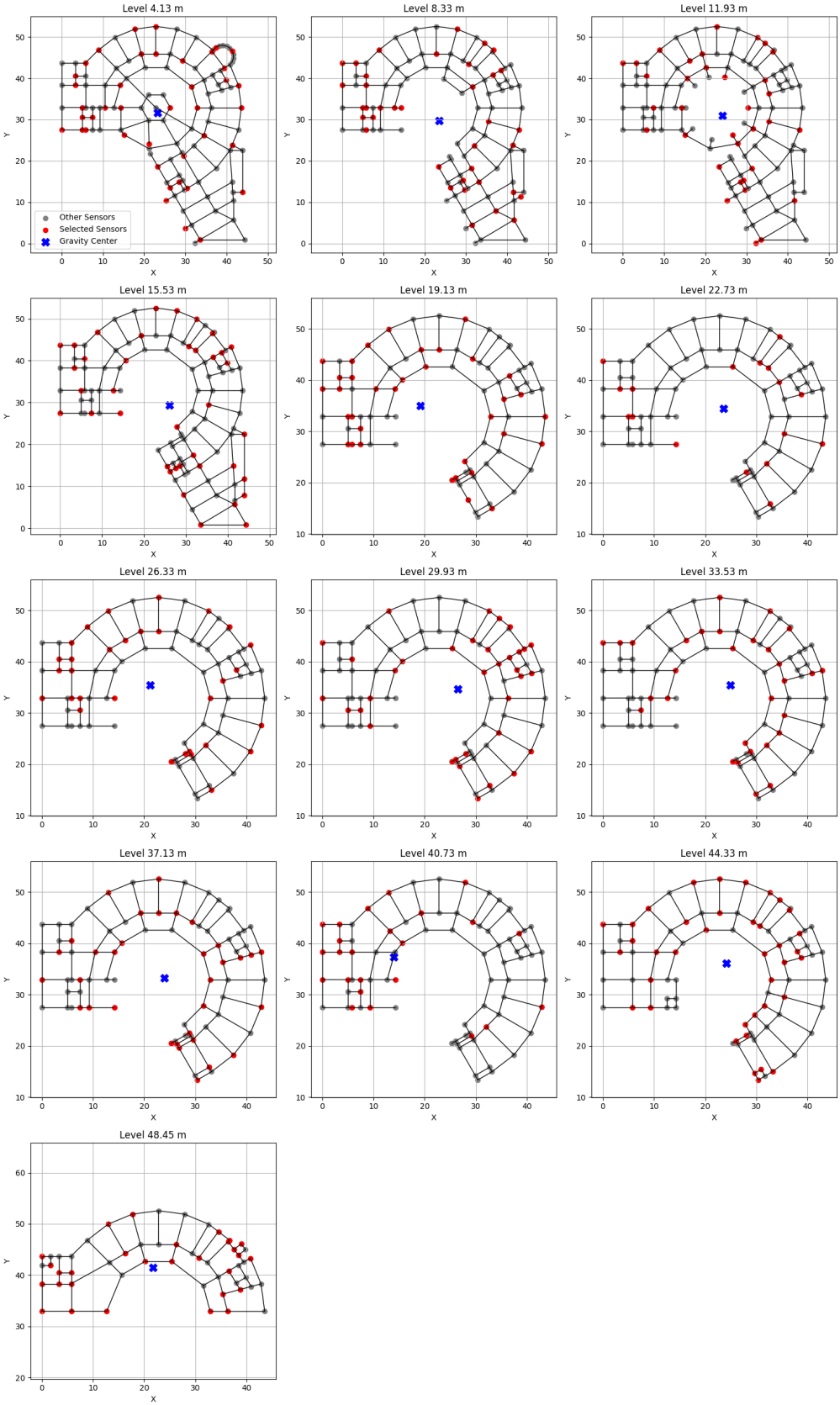


Figure 4.12: Union layout (423 sensors)

### 4.4.5 Custom Layout Selection Methodology

The final sensor configuration was constructed through a structured two-phase algorithm that integrates sensor layouts derived from both damaged and undamaged structural conditions. In the first phase, sensor positions optimized for each damaged zone were gathered from prior simulations assuming localized stiffness degradation. Each zone was associated with a vertical interval, and sensor candidates falling within this span were mapped to corresponding floors.

To handle cases where multiple damage zones influenced the same floor, a floor-wise mutation operator was applied to redistribute sensors and mitigate overpopulation, ensuring efficient spatial utilization without compromising zone coverage.

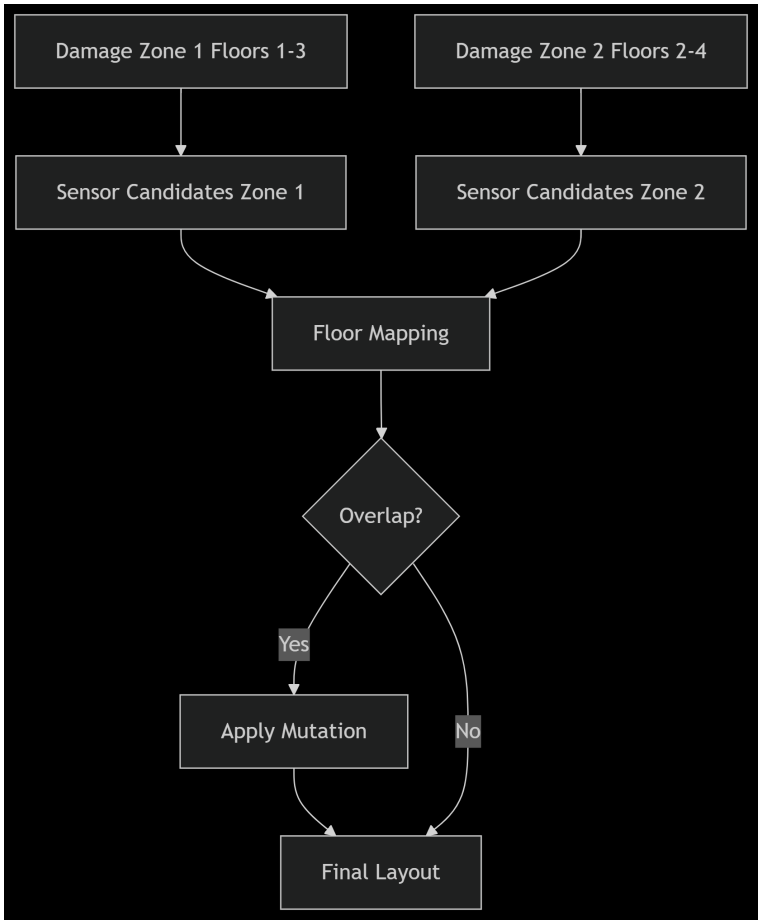


Figure 4.13: Simplified example of the multi-phase sensor layout selection process

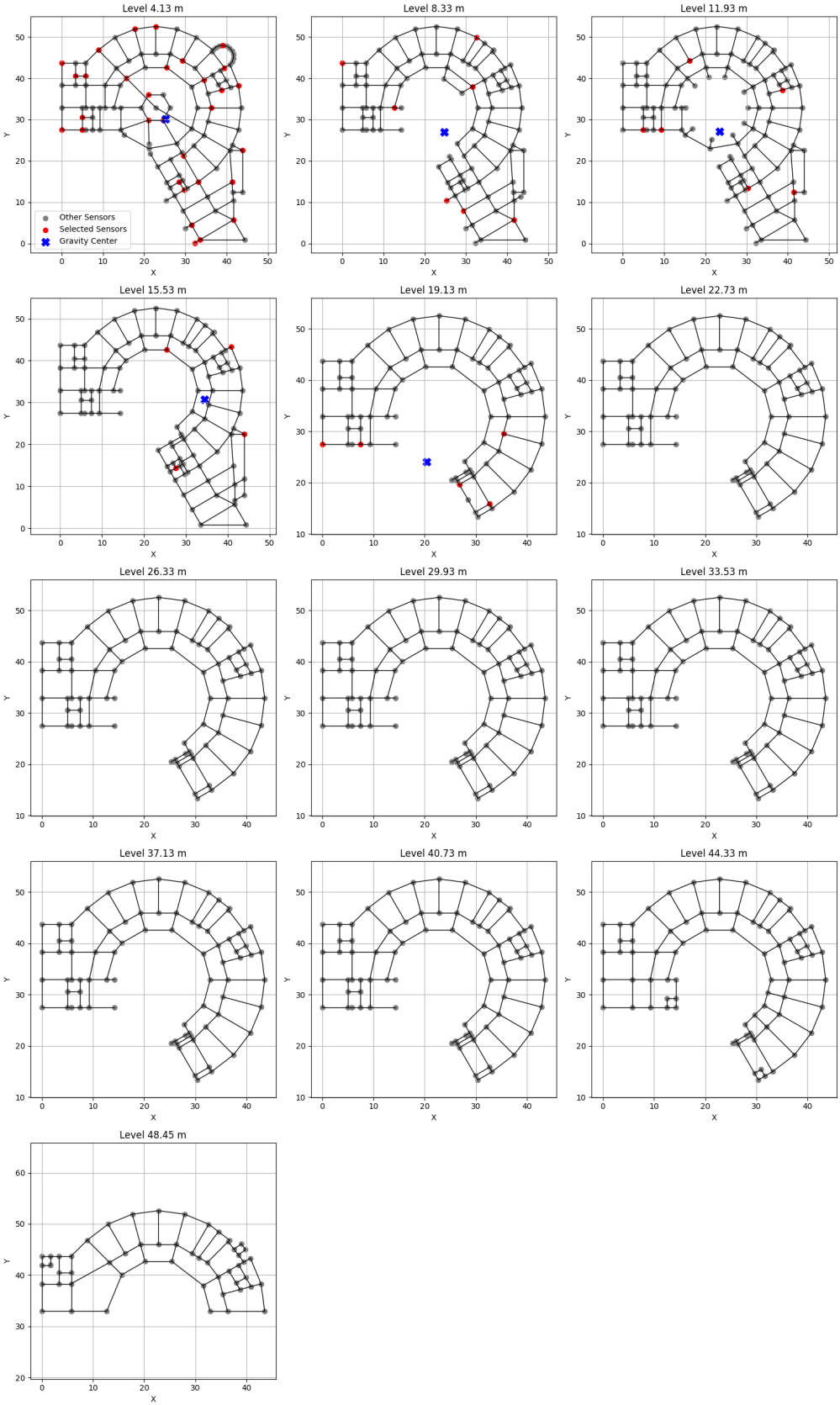


Figure 4.14: Sensor layout prior to Phase 2 (healthy gap filling).

The second phase addressed the remaining floors not assigned sensors during the damage-specific phase. For each such floor, sensors were drawn from a baseline configuration computed under healthy conditions, ensuring that the layout maintained full vertical coverage. This fallback mechanism preserved the global observability of the structure by filling in unmonitored regions with sensors previously identified as informative in the absence of damage.

```
✅ Loaded Z positions for 1130 sensors.
➕ Added 6 healthy sensors to Level Z = 22.73 m
➕ Added 6 healthy sensors to Level Z = 26.33 m
➕ Added 6 healthy sensors to Level Z = 29.93 m
➕ Added 5 healthy sensors to Level Z = 33.53 m
➕ Added 6 healthy sensors to Level Z = 37.13 m
➕ Added 6 healthy sensors to Level Z = 40.73 m
➕ Added 7 healthy sensors to Level Z = 44.33 m
➕ Added 5 healthy sensors to Level Z = 48.45 m

📊 Final Sensor Count per Level:
🏢 Level Z = 4.13 m → 31 sensors
🏢 Level Z = 8.33 m → 7 sensors
🏢 Level Z = 11.93 m → 6 sensors
🏢 Level Z = 15.53 m → 4 sensors
🏢 Level Z = 19.13 m → 5 sensors
🏢 Level Z = 22.73 m → 6 sensors
🏢 Level Z = 26.33 m → 6 sensors
🏢 Level Z = 29.93 m → 6 sensors
🏢 Level Z = 33.53 m → 5 sensors
🏢 Level Z = 37.13 m → 6 sensors
🏢 Level Z = 40.73 m → 6 sensors
🏢 Level Z = 44.33 m → 7 sensors
🏢 Level Z = 48.45 m → 5 sensors

📊 Total unique selected sensors: 100
```

Figure 4.15: Sensor layout immediately before final floorwise mutation phase

The resulting sensor layout thus represents a principled hybrid between damage-aware clustering and healthy-state representativity. It prioritizes critical zones affected by structural degradation while ensuring no floor remains unmonitored. The methodology guarantees that sensor density is elevated in zones of interest and maintains balance across the structure through hierarchical assignment logic rooted in vertical elevation mapping.

Following the initial zone-based sensor aggregation, a significant concentration of sensors was observed at the 4.13 m elevation, resulting in an overcrowded layout with 31 sensors on a single floor. This was addressed through a floor-wise mutation step, which

selectively filtered redundant sensors based on spatial and dynamic similarity. Pairwise XY distances were computed to detect close-proximity sensors, and velocity response vectors were compared, with pairs exhibiting Euclidean distances below a threshold of 1.5 considered functionally redundant. As a result, the sensor count at the 4.13 m level was reduced from 31 to 15, and the overall sensor count decreased from 100 to 84, all while preserving the composite fitness score at 0.754. The refined sensor layout, shown in Figure 4.17, balances monitoring effectiveness with deployment efficiency.

### 4.4.6 Final Sensor Network Configuration

The synthesized 84-sensor network (Fig. 4.17) achieved high coverage efficiency with balanced allocation across structural zones. Key features:

- Non-uniform distribution reflecting structural importance
- Strategic placement near critical load-bearing elements
- Adaptive density based on floor-specific requirements
- Sensor distribution per floor:

| **Floor** | 1 | 2 | 3 | 4 | 5 | 6 | 7 | 8 | 9 | 10 | 11 | 12 | 13 |
|---|---|---|---|---|---|---|---|---|---|---|---|---|---|
| **Sensors** | 15 | 7 | 6 | 4 | 5 | 6 | 6 | 6 | 5 | 6 | 6 | 7 | 5 |

Table 4.9: Sensor Distribution Characteristics

| **Metric** | **Value** |
|---|---|
| Total sensors | 84 |
| Mean per floor | 6.46 |
| Fitness score | 0.754 |
| Ratio metric | 0.0064 |
| Minimum per floor | 4 |
| Maximum per floor | 15 |

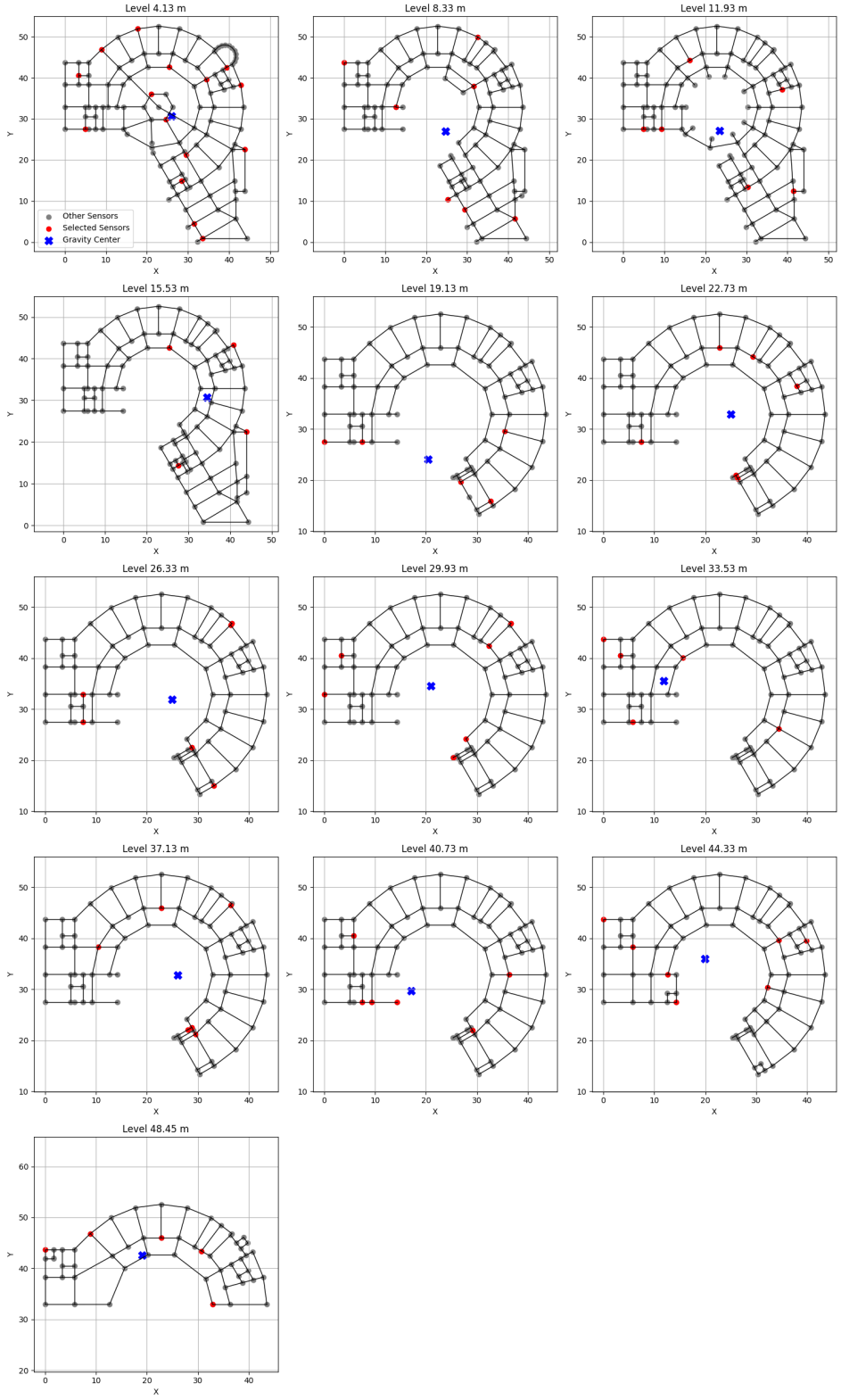


Figure 4.16: Final sensor layout for Tower HQ (4.13m to 48.45m)

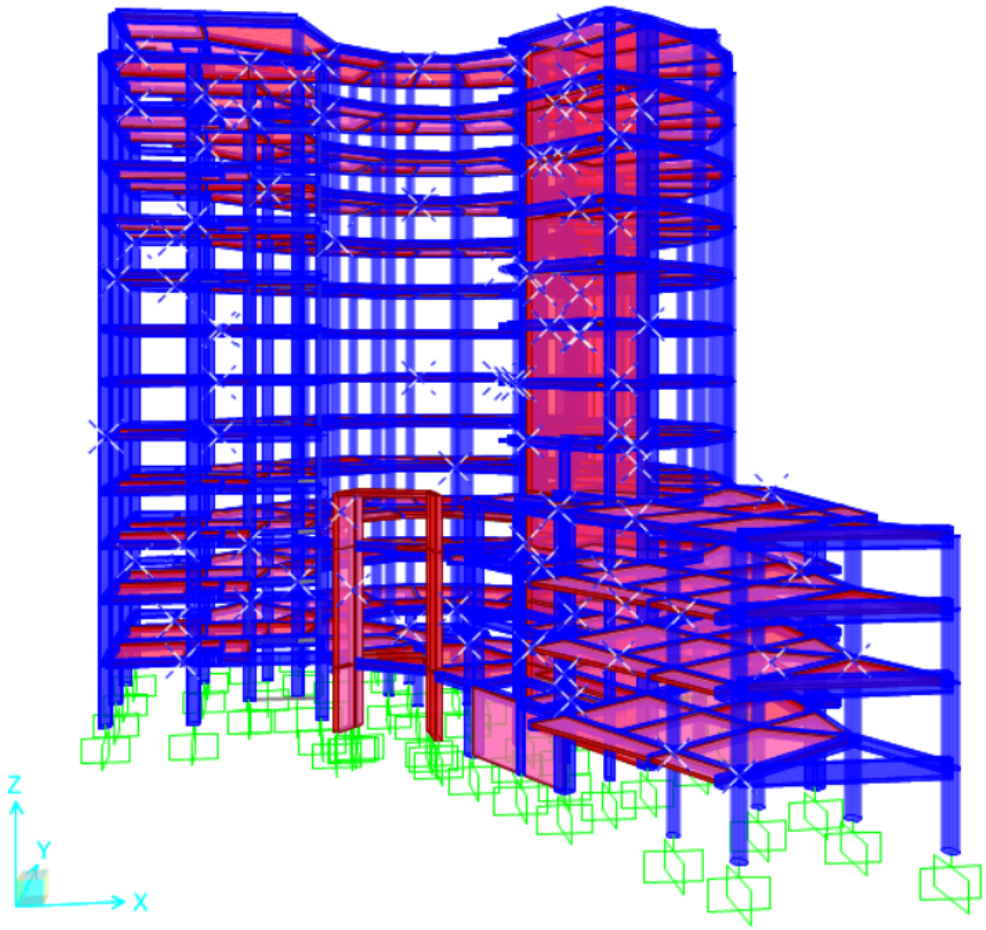


Figure 4.17: Final sensor layout for Tower HQ in 3D Model

## 4.5 Discussion

The sensor optimization study for the COSIDER Headquarters Tower revealed critical insights about structural monitoring in complex medium-rise buildings. The genetic algorithm demonstrated remarkably consistent convergence across all damage scenarios, typically reaching stability within 20 generations as shown in Figure 4.9. This early termination capability reduced computational resources by 80% compared to the maximum 100-generation allocation, suggesting effective exploration of the solution space particularly when using higher mutation rates ($mr = 0.9$) combined with floor-wise mutation ($fw = 1.0$). The three-selection strategy revealed important trade-offs where fitness-optimized solutions consistently delivered the highest damage sensitivity (0.756-0.763),

while performance-to-cost solutions showed minimal fitness degradation (0.749-0.756) with 15-40% more sensors. Notably, minimal-sensor solutions achieved surprisingly high fitness (0.747-0.759) with just 60-71 sensors, challenging conventional sensor density assumptions as demonstrated by Zone 5 detection maintaining 0.759 fitness with only 60 sensors.

The building's irregular geometry significantly impacted optimal placements with shear wall foundations consistently requiring denser coverage, service floors attracting clustered sensors due to stiffness transitions, and top floors proving challenging for consistent coverage. The two-phase placement methodology successfully addressed real-world constraints where the floor-wise mutation operator resolved sensor overcrowding by reducing sensors from 31 to 15 at the 4.13m level, healthy-state gap filling ensured no floor was left unmonitored, and velocity vector filtering effectively eliminated redundant sensors using a fixed threshold of 1.5. The current methodology shows sensitivity to initial population conditions in top-floor optimization and fixed velocity thresholds for redundancy removal, while excluding physical installation constraints. Future enhancements should incorporate adaptive zone-specific filtering thresholds, multi-level refinement algorithms, installation feasibility constraints, and operational vibration testing validation to address these limitations.

## 4.6 Conclusion

This comprehensive case study validates the proposed hybrid SHM framework through application to the 12-story COSIDER Headquarters Tower. Six critical zones were identified through RPA 2024 seismic analysis, with damage realistically simulated via stiffness reduction (0-90%) in SAP2000, representing diverse failure mechanisms from axial column failure to shear wall overturning. The genetic algorithm demonstrated excellent convergence properties, identifying optimal solutions within 20 generations while revealing that high damage sensitivity (0.756-0.763 fitness) is achievable across scenarios, with zone-specific optimization enabling significant sensor reduction down to 60 sensors, and mutation parameters significantly impacting solution quality where $mr = 0.9$ and $fw = 1.0$ proved optimal.

The novel two-phase placement methodology successfully integrated damage-specific prioritization with healthy-state coverage, generating a cost-effective 84-sensor layout shown in Figure 4.17 that maintained high composite fitness (0.754) while resolving over-

crowding and ensuring full vertical coverage through hierarchical assignment. The study confirms that transmissibility-based features coupled with evolutionary optimization provide reliable damage detection in medium-rise RC structures, adaptability to complex geometries and irregular floorplates, and practical solutions balancing sensitivity with implementation cost. The final sensor configuration establishes a foundation for permanent monitoring system installation at the COSIDER Tower, with future work focusing on enhancing robustness under operational variability, developing fault-tolerant network designs, and implementing machine learning-enhanced damage classification systems for critical infrastructure in seismic regions.

# General conclusion

Structural Health Monitoring (SHM) has become an essential field in civil engineering, particularly for buildings subjected to seismic and operational conditions. It enables early detection of structural deterioration, helps prevent critical failures, and extends the service life of structures by supporting informed maintenance decisions. The objective of this thesis was to develop a hybrid methodology for optimizing the number and placement of sensors in mid-rise reinforced concrete buildings, tailored to potential damage scenarios.

The proposed approach is based on transmissibility functions extracted from ambient vibration responses, combined with a dual-mutation genetic algorithm (global and floor-wise). This strategy allows the identification of sensor layouts that concentrate coverage in vulnerable areas while maintaining an efficient use of resources.

The work began with a detailed literature review covering conventional and recent SHM methods, including modal analysis, damage detection indices, and sensor placement optimization. Special attention was given to transmissibility-based techniques due to their applicability under ambient conditions without requiring controlled input forces.

The second chapter presented the optimization methodology using transmissibility distance metrics, supported by steady-state simulations in SAP2000. This was expanded in the following chapter with the introduction of the Damage-Dependent Sensor Network Placement Optimization (DD-SNPO) framework, which explicitly integrates stiffness reduction models to reflect structural degradation.

Finally, the proposed methodology was validated through a case study on the COSIDER Headquarters Tower in Bab Ezzouar, a 12-story reinforced concrete building. Simulated damage scenarios (axial, flexural, and shear failure) demonstrated that sensor placement at mid-height levels and stiffness transition zones was the most effective. The optimized 84-sensor layout achieved similar fitness to the healthy configuration while avoiding the inefficiency of larger sensor networks (e.g., 423 sensors in the union layout).

This hybrid framework—at the intersection of structural modeling, ambient vibration analysis, and AI-driven optimization—offers a practical and scalable solution for smart monitoring of civil structures. It represents a step forward toward adaptive SHM systems capable of evolving with structural conditions and supporting safer, more cost-effective maintenance strategies.

## Perspectives

While the study yields encouraging results, it remains a foundational effort and opens several directions for future research:

- The sensor optimization process could be further refined by expanding the objective function to include additional criteria, such as environmental variability, energy efficiency, or data redundancy.
- Expand the methodology using explainable AI techniques to enhance model transparency and support decision-making.
- Most importantly, field validation on actual structures is essential to confirm the practical relevance and robustness of the proposed methodology. (Conduct on-site validation of the proposed 84-sensor layout on the COSIDER Tower to assess real-world applicability.)

Overall, this work provides a structured and scalable framework for sensor network optimization in seismic-prone reinforced concrete buildings. It contributes to the development of intelligent SHM systems that prioritize efficient resource allocation while remaining adaptable to real-world constraints.

# Bibliography


[1] O. Avci, O. Abdeljaber, S. Kiranyaz, M. Hussein, M. Gabbouj, and D. J. Inman. A review of vibration-based damage detection in civil structures: From traditional methods to machine learning and deep learning applications. *Mechanical systems and signal processing*, 147:107077, 2021.

[2] J. M. Beal, A. Shukla, O. A. Brezhneva, and M. A. Abramson. Optimal sensor placement for enhancing sensitivity to change in stiffness for structural health monitoring. *Optimization and Engineering*, 9:119–142, 2008.

[3] Centre National du Génie Parasismique (CGS). *Règlement Parasismique Algérien RPA 2024*. Alger, Algérie, 2024. Accessed: 2025-07-01.

[4] Y.-J. Cha, W. Choi, and O. Büyüköztürk. Deep learning-based crack damage detection using convolutional neural networks. *Computer-Aided Civil and Infrastructure Engineering*, 32(5):361–378, 2017.

[5] M. Chadha, Y. Yang, Z. Hu, and M. D. Todd. Optimal sensor placement considering operational sensor failures for structural health monitoring applications. In *Society for Experimental Mechanics Annual Conference and Exposition*, pages 89–92. Springer, 2023.

[6] E. J. Cross, S. J. Gibson, M. R. Jones, D. J. Pitchforth, S. Zhang, and T. J. Rogers. *Physics-Informed Machine Learning for Structural Health Monitoring*, pages 347–367. Springer International Publishing, Cham, 2022.

[7] S. W. Doebling, C. R. Farrar, M. B. Prime, and D. W. Shevitz. Damage identification and health monitoring of structural and mechanical systems from changes in their vibration characteristics: a literature review. 1996.

[8] C. R. Farrar and K. Worden. *Structural health monitoring: a machine learning perspective*. John Wiley & Sons, 2012.

[9] M. I. Friswell, J. E. Mottershead, M. Friswell, and J. Mottershead. *Finite element modelling*. Springer, 1995.

[10] M. Ghasemzadeh and A. Kefal. Sensor placement optimization for shape sensing of plates and shells using genetic algorithm and inverse finite element method. *Sensors*, 22(23):9252, 2022.

[11] P. GOMES and S. PEREIRA. Optimal sensor placement for cfrp structures using transmittance functions. *Journal of Vibration Engineering*, 37(2):321–335, 2024.

[12] B. Gunes and O. Gunes. An unsupervised hybrid approach for detection of damage with autoencoder and one-class support vector machine. *Applied Sciences*, 15(8):4098, 2025.

[13] J. Han, H. Zhang, and Z. Hou. Several damage indices based on transmissibility for application in structural damage detection. In *Experimental Vibration Analysis for Civil Structures*, pages 193–202. CRC Press, 2020.

[14] C. Hu and M. T. Afzal. A statistical algorithm for comparing mode shapes of vibration testing before and after damage in timbers. *Journal of Wood Science*, 52:348–352, 2006.

[15] M. KAOULALA and S. OUABDESSELAM. Structural health monitoring strategy for a historic monument: Kalaa de beni hammad. Master's thesis, École Nationale Polytechnique, Algiers, Algeria, 2021. Mémoire de projet de fin d'études.

[16] S. G. R. Kongala. Explainable structural health monitoring (shm) for damage classification based on vibration. Master's thesis, University of Twente, 2024.

[17] M. LAGHOUB and H. KRIDI. Méthode hybride de détection et localisation des dommages : Application sur un pont existant. Master's thesis, École Nationale Polytechnique, Algiers, Algeria, 2020. Projet de fin d'études.

[18] S. M. Lundberg and S.-I. Lee. A unified approach to interpreting model predictions. *Advances in neural information processing systems*, 30, 2017.

[19] I. Makras. Corrosion thickness loss monitoring in marine plates through probabilistic methods. 2024.

[20] H. Sohn. Effects of environmental and operational variability on structural health monitoring. *Philosophical Transactions of the Royal Society A: Mathematical, Physical and Engineering Sciences*, 365(1851):539–560, 2007.

[21] H. Sohn, C. R. Farrar, F. M. Hemez, D. D. Shunk, D. W. Stinemates, B. R. Nadler, and J. J. Czarnecki. A review of structural health monitoring literature: 1996–2001. *Los Alamos National Laboratory, USA*, 1(16):10–12989, 2003.

[22] Z. Sun, M. Mahmoodian, A. Sidiq, S. Jayasinghe, F. Shahrivar, and S. Setunge. Optimal sensor placement for structural health monitoring: A comprehensive review. *Journal of Sensor and Actuator Networks*, 14(2), 2025.

[23] B.-T. Thanh, L.-X. Thang, T.-V. Hung, N.-X. Tung, N.-N. Long, D.-T. Linh, and T. Hoa Ngoc. Damage detection for a cable-stayed bridge under the effect of moving loads using transmissibility and artificial neural network. *Journal of Materials and Engineering Structures «JMES»*, 9(4):411–420, 2022.

[24] K. Worden, C. R. Farrar, G. Manson, and G. Park. The fundamental axioms of structural health monitoring. *Proceedings of the Royal Society A: Mathematical, Physical and Engineering Sciences*, 463(2082):1639–1664, 2007.

[25] T.-H. Yi, H.-N. Li, and M. Gu. Optimal sensor placement for structural health monitoring based on multiple optimization strategies. *The Structural Design of Tall and Special Buildings*, 20(7):881–900, 2011.

[26] R. Zenzen, S. Khatir, I. Belaidi, C. Le Thanh, and M. A. Wahab. A modified transmissibility indicator and artificial neural network for damage identification and quantification in laminated composite structures. *Composite Structures*, 248:112497, 2020.

[27] H. Zhang, Q. Sun, D. Li, C. Li, C. He, and G. Liu. Detecting localized damage in cantilevered structures under nonstationary ambient excitations via gabor spectral mode transmissibility functions. *Scientific Reports*, 14(1):16207, 2024.